Robust Portfolio Selection Problem under Temperature Uncertainty

Nalân Gülpınar, Ethem Çanakoğlu

PII: S0377-2217(16)30383-6
DOI: 10.1016/j.ejor.2016.05.046
Reference: EOR 13732

To appear in: *European Journal of Operational Research*

Received date: 5 May 2015
Revised date: 29 March 2016
Accepted date: 26 May 2016

Please cite this article as: Nalân Gülpınar, Ethem Çanakoğlu, Robust Portfolio Selection Problem under Temperature Uncertainty, *European Journal of Operational Research* (2016), doi: 10.1016/j.ejor.2016.05.046

Highlights

- A portfolio selection problem under temperature uncertainty is studied.
- CVaR portfolio optimization is considered for scenario-based uncertainty set.
- Robust counterparts of the problem are derived using advanced uncertainty sets.
- Risk references are incorporated in the suggested robust framework.
- Computational experiments are presented.

Robust Portfolio Selection Problem under Temperature Uncertainty

Nalân Gülpınar[a], Ethem Çanakoğlu[b]

[a] *The University of Warwick, Warwick Business School, Coventry, CV4 7AL, UK.*
[b] *Bahçeşehir University, Industrial Engineering, Istanbul, Turkey.*

Abstract

In this paper, we consider a portfolio selection problem under temperature uncertainty. Weather derivatives based on different temperature indices are used to protect against undesirable temperature events. We introduce stochastic and robust portfolio optimization models using weather derivatives. The investors' different risk preferences are incorporated into the portfolio allocation problem. The robust investment decisions are derived in view of discrete and continuous sets that the underlying uncertain data in temperature model belong. We illustrate main features of the robust approach and performance of the portfolio optimization models using real market data. In particular, we analyze impact of various model parameters on different robust investment decisions.

Keywords: Robust investment decisions, temperature uncertainty, asset allocation, weather derivatives

1. Introduction

Weather plays a significant role in determining revenue of some industries and market players. National Science Foundation estimated the annual economic impact of weather risk to the US economy as $485 billion in 2011. Various business sectors such as agriculture, retail, tourism and energy are directly affected by exceptional weather conditions (Svec and Stevenson (2007)). For instance, a warm winter may cause excess supplies of oil or natural gas for the utility and energy companies or may incur significant losses in earnings of a winter resort. Similarly, an exceptionally cold summer can affect tourism sector in various aspects. Even big construction companies, especially in Northern Europe, with tight deadlines and costly penalty clauses, consider derivatives to hedge the risk of delays due to weather conditions (The Economist Magazine (2012)).

Weather derivatives were first introduced by Enron in 1997 as financial instruments to minimize effects of climatic events in the US energy industry. Since then, the unregulated market for temperature derivatives has been constantly growing. The standardized contracts are also available in Chicago Mercantile Exchange (CME) for the major cities in the USA, Europe, Australia and Japan. The most common weather derivatives are written on temperature indices that form about 80% of weather contracts to manage weather related risk (Cao and Wei (2004)). There are also weather contracts written on other weather events such as levels of rain, snow, wind, frost and hurricanes.

The pricing problem for weather derivatives has been widely studied in the literature; for instance see Jewson and Brix (2005), Benth and Saltyte-Benth (2007 and 2011), Dorfleitner and Wimmer (2010),

*Corresponding author
Email address: Nalan.Gulpinar@wbs.ac.uk (Nalân Gülpınar)

Schiller et al. (2012), and Hardle et al. (2012). The underlying indices or degree days are modeled under an assumption of various stochastic processes. Garman et al. (2000) and Svec and Stevenson (2007) modeled the underlying indices of weather derivatives using both time series and stochastic approaches. Brody et al. (2002) characterized temperature dynamics by a fractional Ornstein-Uhlenbeck process to price contingent claims based on heating and cooling-degree-days. Hamisultane et al. (2010) studied utility based pricing of weather derivatives. Recently, Elias et al. (2014) compared regime-switching temperature modelling approaches for applications in weather derivatives. The reader is referred to Saltyte-Benth and Benth (2012) for a critical review on temperature modelling.

Weather derivatives have been extensively used as an attractive asset class for hedging and risk management purposes. As Jewson (2004) pointed out, insurance companies, reinsurance companies, banks, hedge funds and energy companies have set up trading desks that are dedicated to weather derivatives. Weather derivatives are traded on different locations for the purpose of insurance over various weather events. Broadly speaking, insurance is designed for low probability extreme events, like hurricanes and tornadoes, whereas weather derivatives are structured for high probability events like a dryer-than-expected summer or warmer-than-expected winter. An insurance payout is only received after a significant loss is proved. On the other hand, a holder of weather derivative contracts receives the payout based on the realization of indices whether they have suffered a loss or not. Turvey (2001) considered weather derivatives as a form of agricultural insurance. Woodard and Garcia (2008) suggested that the potential for weather derivatives in agriculture may be greater, particularly for aggravators of risk such as reinsurer of the agriculture products. Musshoff et al. (2008) investigated portfolio effects and the willingness to pay for weather insurances. Ellithorpe and Punman (2000) stated that participants in the power industry hold a portfolio of weather positions. Brockett (2005) examined the hedging strategies from the credit risk and the basis risk perspectives. Bank and Wiesner (2011) empirically investigated the advantages of using weather derivatives in tourism industry.

The role of weather derivatives within portfolio management has also been recognized by the investment community due to mainly diversification purposes. According to Brockett et al. (2006), investors have seen the potential in weather derivatives as a tool for portfolio diversification, since the derivatives are not expected to correlate significantly with the financial markets. Jewson (2004) highlighted several trading strategies for profitable investment portfolios of weather derivatives. Cao et al. (2004) showed that as an alternative class of financial instruments, weather derivatives can improve the risk-return trade-off in asset allocation decisions. Recently, Barth et al. (2011) studied optimal positions in market-traded temperature futures to hedge spatial risk. The optimal portfolio of futures contracts traded in different locations minimizes the variance with a certain temperature index. In this paper, we introduce a robust optimization approach to portfolio management of weather futures under uncertain temperature. To the best of our knowledge, robust optimization has not been applied to portfolio construction of weather futures and options. The framework laid out in the paper might be of interest to the practitioners for the insurance and risk management purposes.

Robust optimization is considered as an alternative approach to stochastic programming and deals with data uncertainty. Since it was independently developed by Ben-Tal and Nemirovski (1998) and El Ghaoui and Lebret (1997), it has been widely used for solving various stochastic programming problems arising in different sectors such as defence, agriculture, energy, supply chain, healthcare, and finance. The reader is referred to Gorissen et al. (2013) for a detailed overview of robust optimization and its applications in various fields. In particular, it has been applied for robust investment decisions within the single period mean-

variance portfolio allocation framework to handle uncertainty arising due to misspecification and estimation errors for (mainly means and covariance matrices of) random asset returns: for instance see Goldfarb and Iyengar (2003), Ceria and Stubbs (2006), and Kawas and Thiele (2009). Moon and Yao (2011) showed that effective portfolio allocation strategies can be obtained by careful selection of the uncertainty sets over which the worst-case is considered. Soyster and Murphy (2013) introduced a framework for duality and modelling in robust linear programs and applied to the classic Markowitz portfolio selection problem. Oguzsoy and Guven (2007) studied robust portfolio planning problem in the presence of market anomalies. In addition, there exists several successful applications of the robust optimization approach within the multi-period portfolio allocation framework; for instance, see Ben-Tal et al. (2002) and Bertsimas and Pachamanova (2008).

Robust optimization considers the worst-case decision criteria, unlike the expected value criteria is used as a standard approach for decision making problems under uncertainty. It possesses modelling and computational advantages over the stochastic programming, Ben-Tal and El Ghaoui (2009). The data uncertainty is taken into account during modeling stage of the problem without an assumption on specific distribution of the underlying random variables. The uncertain parameters take their worst-case values within a set (so-called an uncertainty set). An uncertainty set consists of general restrictions (representing different forms of rules or factors) on the realizations of the uncertainties of the underlying stochastic program. The robust counterpart of the stochastic program is derived in view of the pre-specified uncertainty set. This is a deterministic model that does not involve an uncertain parameter, Bertsimas et al., (2004). Most importantly, the robust model becomes computationally tractable. The main drawback of the robust optimization methodology is that specific choice of uncertainty sets and budget of robustness may lead to a conservative strategy (Gulpinar and Rustem (2007)). The recent studies showed that data driven robust approaches to design uncertainty sets utilizing data can overcome this issue and avoid overly conservative strategies; see for instance, Bertsimas et al. (2013).

In this paper, we are concerned with a portfolio management problem under temperature uncertainty using weather derivatives. A robust optimization approach to portfolio allocation of weather derivatives is introduced to investigate impact of temperature noise on the investment strategies. We are particularly interested in the effect of robust investment strategies for insurance purposes, that is, whether robust optimization strategies perform better than traditional strategies in extreme scenarios. We present robust formulations of the portfolio allocation problem under different uncertainty sets to incorporate risk preferences of the investor. We therefore consider discrete (scenario-based) as well as continuous (symmetric and asymmetric) uncertainty sets for modelling temperature uncertainty. Specifically, we introduce Conditional Value-at-Risk (CVaR) constraints using scenario-based uncertainty set in the context of portfolio selection problem under weather uncertainty. The symmetric and asymmetric uncertainty sets in view of certain conditions determine a risk measure on the uncertainty arising in the underlying problem. For further information on the use of risk measures in financial applications, the reader is referred to Rockafellar and Uryasev (2000) and Natarajan et al. (2008). The numerical experiments are conducted to analyze performance of different investment strategies determined in view of different risk preferences and to investigate impact of various model parameters on the performance of robust investment decisions using real data.

The rest of the paper is organized as follows. Section 2 presents a brief introduction to weather derivatives and Section 3 focuses on modelling temperature uncertainty. The stochastic portfolio selection problem under

temperature uncertainty is introduced in Section 4. In Section 5, we derive robust portfolio formulations using different uncertainty sets. Section 6 summarizes design of numerical experiments, implementation issues and data analysis . We present an empirical analysis of robust weather investment strategies using real market data and computational results in Section 7. Section 8 concludes the paper with a short summary of findings and future research directions.

2. Weather Derivatives

Weather derivatives are traded as financial instruments between two parties. The seller agrees to bear risk for a premium and makes profit if nothing happens. However, if the weather turns out to be bad, then the buyer claims the agreed amount. Broadly speaking, futures (forwards) and options are main types of weather derivatives that are written on temperature indices. The reader is referred to Jewson (2002) for further discussion on different weather derivatives. Besides the underlying variable of temperature indices, a weather contract must specify such basic elements as the accumulation period, the index location (which records temperatures used to construct the underlying variable), and the tick-size (i.e., fixed lump-sum to be exchanged between parties for each level of degree days). The weather indices are defined through temperature realised at any day for a specific location. The products associated with regions located in the same geographical region are highly correlated. In this sense, a portfolio allocation problem using weather derivatives displays different characteristics from other commodity types such as oil and corn.

We consider weather futures and options based on temperature indices associated with m locations that are indexed by $i, j = 1, \cdots, m$. Let T denote an investment horizon and t represent future discrete time periods, $t = 1, 2, \cdots, T$. We assume that $t = 0$ refers to today. Let $\tilde{H}_{it}$ represent the temperature measured for location $i = 1, \cdots, m$ at time $t = 1, \cdots, T$. The temperature at a specific day is basically average of the highest and lowest temperatures observed during the day.

A degree day is defined as the difference between a reference temperature and the daily observed temperature. The temperature indices are described by heating-degree-days (HDD) and cooling-degree-days (CDD) and cumulative average temperature (CAT). In general terms, the HDD (CDD) indices are used to measure coldness (hotness) of the temperature during a period of November-March (April-November). Let r_i be the reference temperature associated with location i. In general, it is fixed as 18 degrees Celsius or 65 degrees Fahrenheit. The HDD and CDD indices, respectively, at time t for location i are defined as temperatures below and over the reference temperature r_i, and are formulated as

$$HDD(i,t) = \max(r_i - \tilde{H}_{it}, 0), \text{ and } CDD(i,t) = \max(\tilde{H}_{it} - r_i, 0).$$

The total heating and cooling-degree-days for HDD and CDD indices associated with location i over time period T are mathematically formulated as

$$f_i = \sum_{t=1}^{T} HDD(i,t), \text{ and } g_i = \sum_{t=1}^{T} CDD(i,t).$$

In addition, total daily average temperatures with respect to CAT index at location i during the measurement period T is calculated as $d_i = \sum_{t=1}^{T} CAT(i,t) = \sum_{t=1}^{T} \tilde{H}_{it}$.

Let $\bar{f}_i$, $\bar{g}_i$ and $\bar{d}_i$ denote the level of degree days agreed between the parties for HDD, CDD and CAT indices at location i, respectively. A weather futures contract obligates the buyer to purchase the value of underlying temperature index at a future date based on the accumulated heating or cooling-degree-days. The parties exchange the value of the contract at the end of investment horizon. The payoff received from the weather futures contracts on HDD, CDD and CAT temperature indices for location i, respectively, is expressed as

$$F_{HDD}(i) = p_i^h(f_i - \bar{f}_i), \;\; F_{CDD}(i) = p_i^c(g_i - \bar{g}_i), \;\; \text{and} \;\; F_{CAT}(i) = p_i^{ct}(d_i - \bar{d}_i)$$

where p_i^h, p_i^c and p_i^{ct} are tick-sizes attached to HDD, CDD, and CAT indices, respectively, for location i. In the CME market, various weather options written on temperature futures are also traded. A call (put) option provides its owner the right to buy (sell) the underlying asset for a fixed strike price at an agreed exercise time. The underlying asset is a temperature future written on temperature (HDD, CDD or CAT) indices for a specified measurement period.

Let K_i^h and K_i^c denote strike prices of HDD and CDD indices, respectively. The value of a weather call option with underlying futures temperatures written on heating and cooling-degree-days, respectively, for location i is determined as

$$C_{HDD}(i) = p_i^h \max\left(f_i - K_i^h, 0\right), \;\; \text{and} \;\; C_{CDD}(i) = p_i^c \max\left(g_i - K_i^c, 0\right).$$

Similiarly, the value of a weather put option on futures temperatures written on heating and cooling-degree-days for location i can be computed as follows:

$$P_{HDD}(i) = p_i^h \max\left(K_i^h - f_i, 0\right), \;\; \text{and} \;\; P_{CDD}(i) = p_i^c \max\left(K_i^c - g_i, 0\right).$$

Therefore, it is desirable for an investor to exercise the call (put) option when the strike price on the option contract is lower (higher) than the market value of the underlying temperature indices.

Next, we first describe the temperature model based on autoregressive process, and then introduce a stochastic portfolio selection model under temperature uncertainty using weather future derivatives. Weather options can be also included in a similar manner.

3. Modelling Temperature Uncertainty

As mentioned in the introduction, different temperature models have been considered to model weather derivatives in the literature. The reader is referred to Saltyte-Benth and Benth (2012) and references therein for the most recent updates in this area. In particular, Benth and Saltyte-Benth (2005) modelled temperature uncertainty using a discrete mean reverting Ornstein-Uhlenbeck stochastic process and taking into account the correlation information of locations under consideration. The empirical studies indicated that a mean-reverting stochastic process is a reasonable choice for modelling temperature dynamics since temperature gravitates towards its long-run mean. In this paper, following Benth et al. (2008) and Saltyte-Benth and Benth (2012), we consider a general time series model for temperature dynamics. The temperature model consists of different components such as trend line seasonality, autoregressive (AR) process and residual.

We use notation tilde to represent randomness; for example, $(\tilde{*})$ denotes a random variable $(*)$. Let's assume that the trader knows the temperature values today ($t = 0$), but temperature $\tilde{H}_{it}$ for location in future time periods t for $t > 0$ are unknown (uncertain). The temperature dynamics for location i at time t can be modeled as

$$\tilde{H}_{it} = \mu_{it} + \delta_{it}$$

where μ_{it} and δ_{it} represent the mean and the residual process at time t for location i, respectively. As suggested by Saltyte-Benth and Benth (2012), the auto-regressive process AR of order 3 is the best fit for modelling the cyclic component of temperature data. Let l_{ki} for $k = 1, 2, 3$ at location i denote the parameters of $AR(3)$. The mean process is defined in terms of the seasonal and mean reverting components as follows;

$$\mu_{it} = s_{it} + \sum_{k=1}^{3} l_{ki} \left(\tilde{H}_{it-k} - s_{it-k} \right). \tag{1}$$

The seasonal mean function is deterministic and contains a trend and the seasonality of temperature data. It can be formulated as follows;

$$s_{it} = a_{0i} + a_{1i}t + a_{2i} \cos\left(\frac{2\pi \left(t - a_{3i}\right)}{365} \right).$$

The first component (a_{0i}) in the seasonality function of temperature represents the long-term average temperature for location i whereas the trend line ($a_{1i}t$) is used to ensure stationarity in temperature data. A trend could be expressed as an increasing temperature due to for instance, global warming (Saltyte-Benth and Benth (2012)). The trigonometric function in the last component refers the seasonal variation in temperature and changes between the coldest and the warmest periods of the year. The size of variation is equal to two times a_{2i} while a_{3i} denotes the phase variable for the trigonometric function which corresponds to the hottest day in the year.

As shown by the temperature data analysis in Section 6, and also reported in the literature (for instance, see Alaton et al. (2002)), the temperature data suggests that the variability in the residual process δ_{it} is not an independent identically distributed random variable. On the other hand, it depends on the season and also captures correlation of temperatures between all locations (Barth et al. (2011)). Let ρ_{it} be the seasonal variation and $\mathbf{\Sigma}$ represent a $m \times m$ matrix with elements of σ_{ij} where $\mathbf{\Sigma}'\mathbf{\Sigma}$ is the covariance of the normalized residuals.

Therefore, we can model the residual process as

$$\delta_{it} = \rho_{it} \sum_{j=1}^{m} \sigma_{ij} \tilde{\varepsilon}_{jt}. \tag{2}$$

where $\tilde{\varepsilon}_{jt}$ represents independent random noise. The temperature data analysis in Section 6 proves that the noise term follows a distribution with zero mean and 1 standard deviation.

We model the seasonal volatility using Fourier transform function with a single component defined as

$$\rho_{it} = b_{0i} + b_{2i} \cos\left(\frac{2\pi \left(t - b_{3i}\right)}{365} \right).$$

Note that time independent random process exhibit spatial dependence and is used to model the correlation of temperature changes in different locations. This component is modeled as the summation of independent random processes as $\sum_{j=1}^{m} \sigma_{ij}\tilde{\varepsilon}_{jt}$. Therefore, temperature of location i at time t can be rewritten as

$$\tilde{H}_{it} = s_{it} + \sum_{k=1}^{3} l_{ki}\left(\tilde{H}_{i,t-k} - s_{i,t-k}\right) + \rho_{it}\sum_{j=1}^{m}\sigma_{ij}\tilde{\varepsilon}_{jt}.$$

Let's assume that the temperature values for 3 days prior to current day, $H_{i(-2)}, H_{i(-1)}, H_{i(0)}$, and seasonal components for that period, $s_{i(-2)}, s_{i(-1)}, s_{i(0)}$, for location i are known. Using the backward induction and some algebra, one can obtain the temperature at time t for location i as a function of the temperatures at the beginning of decision period (namely, $H_{i(-2)}, H_{i(-1)}$, and $H_{i(0)}$) and can be written as follows:

$$\tilde{H}_{it} = s_{it} + \sum_{k=1}^{3} A_{it}^{k}\left(H_{i(1-k)} - s_{i(1-k)}\right) + \sum_{k=1}^{t} A_{i(t-k)}^{1}\rho_{it}\sum_{j=1}^{m}\sigma_{ij}\tilde{\varepsilon}_{jk}, \tag{3}$$

where $A_{it}^{1} = \sum_{\forall a+2b+3c=t} l_{1i}^{a} l_{2i}^{b} l_{3i}^{c}$, $A_{it}^{2} = A_{i(t+1)}^{1} - A_{it}^{1} l_{1i}$, and $A_{it}^{3} = A_{i(t+2)}^{1} - A_{i(t)}^{1} l_{2i} - A_{i(t+1)}^{2} l_{1i}$. The total heating-degree-days for HDD and CDD temperature indices over a planning horizon T are computed as

$$f_i = \sum_{t=1}^{T} \max\left(r_i - s_{it} - \sum_{k=1}^{3} A_{it}^{k}\left(H_{i(1-k)} - s_{i(1-k)}\right) - \sum_{k=1}^{t} A_{i(t-k)}^{1}\rho_{it}\sum_{j=1}^{m}\sigma_{ij}\tilde{\varepsilon}_{jk},\ 0\right), \text{ and} \tag{4}$$

$$g_i = \sum_{t=1}^{T} \max\left(s_{it} + \sum_{k=1}^{3} A_{it}^{k}\left(H_{i(1-k)} - s_{i(1-k)}\right) + \sum_{k=1}^{t} A_{i(t-k)}^{1}\rho_{it}\sum_{j=1}^{m}\sigma_{ij}\tilde{\varepsilon}_{jk} - r_i,\ 0\right). \tag{5}$$

4. Stochastic Portfolio Allocation under Temperature Uncertainty

We assume that an investor (a firm, a hedge fund or an insurance company) is concerned with weather risk and wishes to construct a portfolio using weather derivatives traded in the CME market. Moreover, the investor considers two types of futures contracts in the market where temperature is the underlying index for weather futures (written on HDD and CDD temperature indices over a given measurement period). Let x_i^h and x_i^c be decision variables representing weights of the futures contracts written on heating and cooling-degree indices for location i, respectively. The capital is normalized to unity so that we have

$$\sum_{i=1}^{m} x_i^h + x_i^c = 1 \tag{6}$$

where non-negativity constraints on asset weights, $x_i^h,\ x_i^c \geq 0$ for $i = 1, \cdots, m$ aim to avoid the short-sale. The expected terminal wealth obtained from an investment of weather futures written on HDD and CDD temperature indices for location i is computed as

$$E\left[x_i^h p_i^h\left(f_i - \bar{f}_i\right) + x_i^c p_i^c\left(g_i - \bar{g}_i\right)\right]$$

Recall that p_i^h and p_i^c define the tick sizes for HDD and CDD contracts, respectively. The investor's goal is to maximize the total expected wealth that is achieved by the investment on HDD and CDD weather futures associated with locations $i = 1, \cdots, m$. Then the stochastic portfolio allocation problem can be formulated as follows;

$$
\begin{aligned}
P_{nom}: \quad \max_{x_i^h, x_i^c} \quad & \sum_{i=1}^{m} E\left[x_i^h p_i^h \left(f_i - \bar{f}_i\right) + x_i^c p_i^c \left(g_i - \bar{g}_i\right)\right] \\
\text{s.t.} \quad & f_i = \sum_{t=1}^{T} \max\left(r_i - s_{it} - \sum_{k=1}^{3} A_{it}^k \left(H_{i(1-k)} - s_{i(1-k)}\right) - \sum_{k=1}^{t} A_{i(t-k)}^1 \rho_{it} \sum_{j=1}^{m} \sigma_{ij} \tilde{\varepsilon}_{jk},\ 0\right), \\
& \qquad\qquad\qquad\qquad\qquad\qquad\qquad\qquad\qquad\qquad\qquad\qquad i = 1, \cdots, m \\
& g_i = \sum_{t=1}^{T} \max\left(s_{it} + \sum_{k=1}^{3} A_{it}^k \left(H_{i(1-k)} - s_{i(1-k)}\right) + \sum_{k=1}^{t} A_{i(t-k)}^1 \rho_{it} \sum_{j=1}^{m} \sigma_{ij} \tilde{\varepsilon}_{jk} - r_i,\ 0\right), \\
& \qquad\qquad\qquad\qquad\qquad\qquad\qquad\qquad\qquad\qquad\qquad\qquad i = 1, \cdots, m \\
& \sum_{i=1}^{m} x_i^h + x_i^c \ = 1 \\
& x_i^h \geq 0, \quad x_i^c \geq 0, \qquad\qquad i = 1, \cdots, m.
\end{aligned}
$$

Notice that f_i and g_i functions (in the first and second sets of equations) are written explicitly rather than substituting in the objective function due to convenience since the uncertain parameters arising in these equations will be robustified in the upcoming sections.

The solution of the single-period portfolio selection model with recourse determines an optimal allocation of wealth among temperature derivatives written on heating and cooling indices. The optimal investment decision is made at the beginning of the investment horizon and total wealth received from the investment depends on the path the temperature following between today $t = 0$ and final time period T like some exotic options. As mentioned earlier, a stochastic programming model assumes that the decision maker is concerned with the average performance of the system. Moreover, it requires a known distribution of the underlying uncertainty. The expected wealth, formulated in terms of contributions of weather futures under consideration, in P_{nom} can be easily computed by estimating expected return of each weather futures under an assumption of specific noise distribution. Then the stochastic programming model above becomes a simple linear programming problem that supplies the investment strategy to achieve maximum portfolio return. Similarly, we can construct a scenario-based stochastic programming model to maximize the expected wealth with discrete number of future temperature scenarios that are generated by the underlying distribution of random parameters. Both approaches provide risk-neutral strategies. On the other hand, for the risk-seeking investment decisions, the expected risk needs to be specifically modeled and minimized for the optimal portfolio allocation. In this paper, we consider conditional Value-at-Risk (CVaR) metric and analyze the risk factor for CVaR constraints in the context of temperature risk management. The alternative risk preferences of the investor will be imposed through robust approaches in the next section.

Following Rockafellar and Uryasev (2000), the Conditional Value-at-Risk measure for a random variable $\tilde{v}$, $\rho_{1-\epsilon}(\tilde{v})$, is defined as

$$
\rho_{1-\epsilon}(\tilde{v}) = \min_{a} \left\{ a + \frac{1}{\epsilon} E(-\tilde{v} - a)^+ \right\},
$$

that can be reformulated by a set of the CVaR constraints in view of N discrete scenarios of $\tilde{v}$ as

$$U_{cvar}(v) = \left\{ \mu + \frac{1}{\lfloor (1-\delta)\cdot N \rfloor} \sum_{n=1}^{N} \beta_n \leq C_\delta, \;\; -\mu - \beta_n \leq f(\tilde{v}), \;\; \beta_n \geq 0, \;\; n = 1, \ldots, N \right\}$$

where $\lfloor \cdot \rfloor$ denotes the integer part of a real number and C_δ is a predetermined constant and $f(\tilde{v})$ is the loss function. It is worthwhile to mention that the set of CVaR constraints constructs a scenario-based uncertainty set in the context of robust optimization; for instance see Bertsimas et al. (2013).

The CVaR portfolio optimization model under weather derivatives considers K realisations of random temperature. For each realisation $\bar{k} = 1, \ldots, K$ and futures $i = 1, \cdots, m$, we can compute $\gamma_i^{\bar{k}}$, and $\delta_i^{\bar{k}}$ as follows;

$$\gamma_i^{\bar{k}} = \sum_{t=1}^{T} \max \left(r_i - s_{it} - \sum_{k=1}^{3} A_{it}^{k} \left(H_{i(1-k)} - s_{i(1-k)} \right) - \sum_{k=1}^{t} A_{i(t-k)}^{1} \rho_{it} \sum_{j=1}^{m} \sigma_{ij} \varepsilon_{jk}^{\bar{k}}, \; 0 \right), \quad \text{and}$$

$$\delta_i^{\bar{k}} = \sum_{t=1}^{T} \max \left(s_{it} + \sum_{k=1}^{3} A_{it}^{k} \left(H_{i(1-k)} - s_{i(1-k)} \right) + \sum_{k=1}^{t} A_{i(t-k)}^{1} \rho_{it} \sum_{j=1}^{m} \sigma_{ij} \varepsilon_{jk}^{\bar{k}} - r_i, \; 0 \right).$$

The expected portfolio return over K scenarios must be at least at the target level W_{target}. This condition is basically formulated as follows:

$$\sum_{\bar{k}=1}^{K} \frac{1}{K} \sum_{i=1}^{m} x_i^h p_i^h \left(\gamma_i^{\bar{k}} - \bar{f}_i \right) + x_i^c p_i^c \left(\delta_i^{\bar{k}} - \bar{g}_i \right) \geq W_{target}.$$

The CVaR portfolio allocation problem with conditional performance constraint on weather derivatives can be formulated as follows:

$$\begin{aligned}
P_{cvar}: \quad & \min \; \Gamma \\
& \text{s.t.} \quad \mu + \frac{1}{\lfloor (1-\beta)\cdot K \rfloor} \sum_{\bar{k}=1}^{K} u_{\bar{k}} \leq \Gamma, \\
& \qquad u_{\bar{k}} \geq -\sum_{i=1}^{m} \left[x_i^h p_i^h \left(\gamma_i^{\bar{k}} - \bar{f}_i \right) + x_i^c p_i^c \left(\delta_i^{\bar{k}} - \bar{g}_i \right) \right] - \mu, \qquad \bar{k} = 1, \ldots, K \\
& \qquad \sum_{\bar{k}=1}^{K} \frac{1}{K} \sum_{i=1}^{m} x_i^h p_i^h \left(\gamma_i^{\bar{k}} - \bar{f}_i \right) + x_i^c p_i^c \left(\delta_i^{\bar{k}} - \bar{g}_i \right) \geq W_{target}, \\
& \qquad u_{\bar{k}} \geq 0, \;\; x_i^c \geq 0, \;\; x_i^h \geq 0 \qquad\qquad i = 1, \cdots, m, \;\; \bar{k} = 1, \ldots, K.
\end{aligned}$$

The CVaR minimization (or maximization) model imposes single objective to find an optimal investment strategy for minimum risk (or maximum wealth) portfolio in view of risk preferences of the investor. The multi-objective formulation produces a minimum risk investment strategy to achieve pre-determined wealth W_{target}. Notice that P_{cvar} is a linear programming model whose size (in terms of number of constraints and variables) depends on the number of assets as well as the number of scenarios generated.

Next, we introduce a tractable approach to determining robust investment strategies using weather derivatives. For a decision maker who is concerned with the worst-case performance of the system, or

probabilistic guarantees on the optimal solution, robust optimization may be a plausible approach since it takes into account investors' risk preferences and provides a guaranteed performance at the worst-case.

5. Robust Investment Decisions using Weather Contracts

We assume that uncertain parameters $\tilde{\varepsilon}_t$ vary within an uncertainty set $\mathfrak{U}_\varepsilon$. The robust counterpart of the stochastic portfolio management problem optimizes the worst-case wealth over a given uncertainty set for the random variables and can be formulated as

$$
\begin{aligned}
P_{rob}: \max_{x_i^h, x_i^c} \min_{\tilde{\varepsilon}_{it} \in \mathfrak{U}_\varepsilon} & \sum_{i=1}^{m} \left(x_i^h p_i^h \sum_{t=1}^{T} \gamma_{it} + x_i^c p_i^c \sum_{t=1}^{T} \delta_{it} - x_i^h p_i^h \bar{f}_i - x_i^c p_i^c \bar{g}_i \right) \\
\text{s.t.} \quad & \gamma_{it} = \max\left(r_i - s_{it} - \sum_{k=1}^{3} A_{it}^k \left(H_{i(1-k)} - s_{i(1-k)} \right) - \sum_{k=1}^{t} A_{i(t-k)}^1 \rho_{it} \sum_{j=1}^{m} \sigma_{ij} \tilde{\varepsilon}_{jk},\ 0 \right), \quad i = 1, \cdots, m, \\
& \qquad t = 1, \cdots, T \\
& \delta_{it} = \max\left(s_{it} + \sum_{k=1}^{3} A_{it}^k \left(H_{i(1-k)} - s_{i(1-k)} \right) + \sum_{k=1}^{t} A_{i(t-k)}^1 \rho_{it} \sum_{j=1}^{m} \sigma_{ij} \tilde{\varepsilon}_{jk} - r_i,\ 0 \right), \quad i = 1, \cdots, m, \\
& \qquad t = 1, \cdots, T \\
& \sum_{i=1}^{m} x_i^h + x_i^c = 1, \quad x_i^h \geq 0, \quad x_i^c \geq 0, \qquad i = 1, \cdots, m.
\end{aligned}
$$

The $\max(a, 0)$ function (in the first and second sets of constraints of the minimax problem above) takes either positive value of function a or zero. Therefore, it can be represented by a constraint as $y \geq a$ where $y \geq 0$. Let Γ be a free variable representing the worst-case portfolio wealth in view of $\tilde{\varepsilon}_{it} \in \mathfrak{U}_\varepsilon$. We can show that the optimization problem above is equivalent to

$$
\begin{aligned}
\max_{x_i^h, x_i^c, \Gamma} \quad & \Gamma - \sum_{i=1}^{m} x_i^h p_i^h \bar{f}_i - x_i^c p_i^c \bar{g}_i \\
\text{s.t.} \quad & \Gamma \geq \sum_{i=1}^{m} \sum_{t=1}^{T} x_i^h p_i^h \gamma_{it} + x_i^c p_i^c \delta_{it}, \\
& \gamma_{it} \geq r_i - s_{it} - \sum_{k=1}^{3} A_{it}^k \left(H_{i(1-k)} - s_{i(1-k)} \right) - \sum_{k=1}^{t} A_{i(t-k)}^1 \rho_{it} \sum_{j=1}^{m} \sigma_{ij} \tilde{\varepsilon}_{jk}, \quad i = 1, \cdots, m, \\
& \qquad t = 1, \cdots, T \\
& \delta_{it} \geq s_{it} + \sum_{k=1}^{3} A_{it}^k \left(H_{i(1-k)} - s_{i(1-k)} \right) + \sum_{k=1}^{t} A_{i(t-k)}^1 \rho_{it} \sum_{j=1}^{m} \sigma_{ij} \tilde{\varepsilon}_{jk} - r_i, \quad i = 1, \cdots, m, \\
& \qquad t = 1, \cdots, T \\
& \tilde{\varepsilon}_{it} \in \mathfrak{U}_\varepsilon, \qquad \gamma_{it},\ \delta_{it} \geq 0, \qquad i = 1, \cdots, m, \qquad t = 1, \cdots, T \\
& \sum_{i=1}^{m} x_i^h + x_i^c = 1, \qquad x_i^h \geq 0, \quad x_i^c \geq 0, \qquad i = 1, \cdots, m.
\end{aligned}
$$

The worst-case outcome of the stochastic data $\tilde{\varepsilon}_{it}$ within a pre-specified uncertainty set $\mathfrak{U}_\varepsilon$ is derived and the corresponding representation of each uncertain coefficient is reinjected into the original problem to obtain its robust counterpart. This is typically a deterministic problem and does not involve random

parameters. The important issue is how to construct an uncertainty set so that random behaviour of the data is well captured, and, at the same time, its robust counterpart should be solved efficiently, in the most computationally tractable way. As Bertsimas et al. (2004) highlighted, an uncertainty set can be determined by statistical estimates and probabilistic guarantees for the solution. The random data that belongs to an uncertainty set is mapped out from the probability distribution of uncertain factors. The support of the random variables can be approximated by using different shapes of the uncertainty sets such as ellipsoidal, box and polyhedral that have been widely used in different applications in the literature. In this paper, we consider symmetric (ellipsoidal) and asymmetric uncertainty sets (introduced by Chen et al. (2007)) to find the corresponding robust counterpart of the asset allocation problem in the context of risk management. The CVaR optimization approach under the scenario-based uncertainty set takes into account the investor's risk preferences. Recall that the scenario-based uncertainty set, that is already defined (in Section 4) for the CVaR risk optimization model, will be used as a benchmark to compare with the performance of risk-seeking investors' robust strategies.

It is worthwhile to mention that the size and shape of the uncertainty sets play an important role on performance of the robust strategies. The size of the uncertainty set is often related to guarantees on the probability that the constraint involving uncertain coefficients will not be violated. There is a trade-off between the amount of protection against uncertainty that is desired and optimality - the smaller the probability that the constraint will be violated, the more the modeller gives up in terms of optimality of the robust solution relative to the solution to the original optimization problem.

The shape of the uncertainty set defines a risk measure on the constraints with uncertain coefficients; for instance, see Natarajan et al. (2009). In practice, the shape is selected to reflect the modeler's knowledge of the probability distributions of the uncertain parameters, while at the same time making the robust counterpart problem efficiently solvable. The symmetric (e.g. ellipsoidal) uncertainty set defines a standard-deviation-like risk measure on the constraint with uncertain parameters. The uncertainty sets with a specific asymmetric shape that incorporates knowledge about the skewed probability distributions of the underlying random asset returns, can improve the performance of investment decisions under Value-at-Risk type risk measures on the portfolio return (Natarajan et al. (2008)). On the other hand, a symmetric uncertainty set with an ellipsoidal shape can be interpreted as variance type risk measures (Fabozzi et al. 2007).

We now focus on robust formulations of the portfolio allocation problem for weather derivatives using symmetric and asymmetric uncertainty sets.

Symmetric Uncertainty Set: In general terms, an ellipsoidal uncertainty set describes a distance requirement - the form of the Euclidean norm - between all elements of the set and the point estimates of the uncertain data. For random variables $\tilde{\varepsilon}_t = [\tilde{\varepsilon}_{1t}, \tilde{\varepsilon}_{2t}, \cdots, \tilde{\varepsilon}_{mt}]$, we can mathematically define ellipsoidal uncertainty set $\mathcal{U}_{\mathcal{E}}$ as

$$\mathcal{U}_{\mathcal{E}} = \left\{ \tilde{\varepsilon}_t \mid \left\| \mathbf{Q}^{-1/2} \left(\tilde{\varepsilon}_t - \hat{\varepsilon}_t \right) \right\|_2 \leq \kappa \right\}, \tag{7}$$

where matrix $\mathbf{Q}$ denotes an estimated covariance matrix and $\hat{\varepsilon}_{\mathbf{t}}$ is an expected value of the distribution of random variables $\tilde{\varepsilon}_t$. In addition, radius κ measures the level of the robustness (sometimes referred to as the "robustness budget" or the "price of robustness"). The size of uncertainty set (as defined by κ parameter) describes a condition on the probability of the constraint (involving uncertain coefficients) feasibility. The smaller κ value indicates less protection against uncertainty that means more giving up in terms of robustness

of the solution for the underlying problem.

For random variables $\tilde{\varepsilon}_t = \{\tilde{\varepsilon}_{1t}, \tilde{\varepsilon}_{2t}, \cdots, \tilde{\varepsilon}_{mt}\}$, at time period $t = 1, \cdots, T$, we have $\hat{\varepsilon}_{\mathbf{t}} = 0$ and $\mathbf{Q} = \mathbf{I}$. In this case, the ellipsoidal set for error terms at time t is simplified as $\mathcal{U}_{\mathcal{E}} = \{\tilde{\varepsilon}_{it} : \|\tilde{\varepsilon}_t\|_2 \leq \kappa\}$. Let α_{it} and β_{it} be Lagrangian multipliers associated with constraints in R_{nom}. In addition, let's define a vector $\mathbf{B_t}$ of $B_t(i) = \sum_{k=t}^{T} (\alpha_{ik} - \beta_{ik})\, A^1_{i(t-k)} \rho_{it}$ for $i = 1, \cdots, m$ and $t = 1, \cdots, T$. The robust counterpart of the underlying stochastic program using the ellipsoidal uncertainty set can be derived as in the following theorem.

Theorem 1. *The robust counterpart of the portfolio allocation problem under the symmetric uncertainty set using futures weather contracts with heating and cooling-degree-days can be formulated as*

$$
\begin{aligned}
R_{sym}: \quad \max \quad & \Pi - \sum_{i=1}^{m} \left(x_i^h p_i^h \bar{f}_i + x_i^c p_i^c \bar{g}_i \right) \\
s.t. \quad & \sum_{i=1}^{m} \sum_{t=1}^{T} (\alpha_{it} - \beta_{it}) \left(r_i - s_{it} - \sum_{k=1}^{3} A_{it}^k \left(H_{i(1-k)} - s_{i(1-k)} \right) \right) - \kappa \sum_{t=1}^{T} \|\mathbf{\Sigma_t} \mathbf{B}_t\|_2 \geq \Pi \\
& \sum_{i=1}^{m} x_i^h + x_i^c = 1 \\
& x_i^h p_i^h - \alpha_{it} \geq 0, \qquad i = 1, \cdots, m, \;\; t = 1, \cdots, T \\
& x_i^c p_i^c - \beta_{it} \geq 0, \qquad i = 1, \cdots, m, \;\; t = 1, \cdots, T \\
& x_i^h \geq 0, \quad x_i^c \geq 0, \qquad i = 1, \cdots, m \\
& \alpha_{it}, \beta_{it} \geq 0, \qquad i = 1, \cdots, m, \;\; t = 1, \cdots, T.
\end{aligned}
$$

As shown in Appendix B, a formal proof of Theorem 1 derives the robust counterpart of the corresponding problem. This process requires to solve (inner) optimization problems that find the worst-case values of the terms involving uncertain coefficients when these uncertain coefficients vary in the uncertainty sets. Notice that in case of the ellipsoidal uncertainty sets with zero means and the unity covariance matrices of the uncertain error coefficients, the robust counterparts of the constraints involve the square root terms. Therefore, the robust portfolio allocation model is a second-order-cone programming problem. An explanation of the specific optimization setup used for numerical experiments will be provided in Section 6.

The computational experience shows that symmetric uncertainty sets for the uncertain asset returns in the portfolio optimization problem could lead to a highly conservative strategy, especially when the random parameters possess skewed distributions, Ceria and Stubbs (2006). In other words, the asymmetric characteristics of distribution may not be well captured by the symmetric uncertainty set. In order to deal with this issue, Chen et al. (2007) introduced an asymmetric uncertainty set using a factor-based model to represent forward and backward deviations of the random variables in the underlying application. They showed that the asymmetric uncertainty set represents a generic convex uncertainty set (ellipsoidal) when the underlying random variable follows a normal distribution. Next, we will give a brief overview of this approach and present the robust formulation of the portfolio management of weather derivatives using an asymmetric uncertainty set in the following theorem.

Asymmetric Uncertainty Set: Let $\tilde{\mathbf{z}}_{\mathbf{t}}$ be independent random factors with zero mean and $\mathbf{\Xi}_t$ denote the covariance matrix of $\hat{\varepsilon}_{\mathbf{t}}$. Following Chen et al. (2007), we consider a factor model $\tilde{\varepsilon}_{\mathbf{t}} = \hat{\varepsilon}_{\mathbf{t}} + (\mathbf{\Xi_t})^{\frac{1}{2}} \tilde{\mathbf{z}}_{\mathbf{t}}$ for the error terms (temperature noise) arising in the future derivatives. Let's define $\phi_j > 0$ and $\psi_j > 0$, $j = 1, \cdots, m$, to denote the forward and backward deviations of random variable $\tilde{\mathbf{z}}_{\mathbf{t}}$, respectively, and define

diagonal matrices $\mathbf{P} = diag(\phi_{1t}, \cdots, \phi_{mt})$ and $\mathbf{R} = diag(\psi_{1t}, \cdots, \psi_{mt})$. In addition, decompose the random variable $\tilde{\mathbf{z}}_\mathbf{t}$ into two random variables $\tilde{\mathbf{v}}_\mathbf{t}$ and $\tilde{\mathbf{w}}_\mathbf{t}$ such that $\tilde{\mathbf{z}}_\mathbf{t} = \tilde{\mathbf{v}}_\mathbf{t} - \tilde{\mathbf{w}}_\mathbf{t}$ where $\tilde{\mathbf{v}}_\mathbf{t} = \max\{\tilde{\varepsilon}_\mathbf{t}, 0\}$ and $\tilde{\mathbf{w}}_\mathbf{t} = \max\{-\tilde{\varepsilon}_\mathbf{t}, 0\}$. Both $\tilde{\mathbf{v}}_\mathbf{t}$ and $\tilde{\mathbf{w}}_\mathbf{t}$ are positive and at least one of them is zero. Using a finite distribution support for the random variables, $[-\underline{\mathbf{z}}_\mathbf{t},\ \bar{\mathbf{z}}_\mathbf{t}]$, the asymmetric uncertainty set is described as

$$\mathcal{U}_A = \left\{\tilde{\mathbf{z}}_\mathbf{t} :\ \exists \tilde{\mathbf{v}}_\mathbf{t},\ \tilde{\mathbf{w}}_\mathbf{t} \in R^m,\ \tilde{\mathbf{z}}_\mathbf{t} = \tilde{\mathbf{v}}_\mathbf{t} - \tilde{\mathbf{w}}_\mathbf{t},\ ||\mathbf{P}^{-1}\tilde{\mathbf{v}}_\mathbf{t} + \mathbf{R}^{-1}\tilde{\mathbf{w}}_\mathbf{t}|| \leq \Omega,\ -\underline{\mathbf{z}}_\mathbf{t} \leq \tilde{\mathbf{z}}_\mathbf{t} \leq \bar{\mathbf{z}}_\mathbf{t}\right\}.$$

Theorem 2. *The robust counterpart of the portfolio allocation problem under the asymmetric uncertainty set using futures weather contracts with temperature indices can be formulated as follows;*

$$\begin{aligned}
R_{asym}: \quad \max \quad & \Upsilon - \sum_{i=1}^{m} x_i^h p_i^h \bar{f}_i + x_i^c p_i^c \bar{g}_i \\
s.t. \quad & \sum_{i=1}^{m}\sum_{t=1}^{T} (\alpha_{it} - \beta_{it}) \left(r_i - s_{it} - \sum_{k=1}^{3} A_{it}^k \left(H_{i(1-k)} - s_{i(1-k)} \right) \right) - \Omega \sum_{t=1}^{T} \|\mathbf{u}_\mathbf{t}\|_2 \geq \Upsilon, \\
& u_{it} \geq \psi_i \sum_{k=t}^{T} A_{i(t-k)}^1 \rho_{it} \sum_{j=1}^{m} \sigma_{ij} (\alpha_{it} + \beta_{it}), && i = 1, \cdots, m, \quad t = 1, \cdots, T \\
& u_{it} \geq \phi_i \sum_{k=t}^{T} A_{i(t-k)}^1 \rho_{it} \sum_{j=1}^{m} \sigma_{ij} (\alpha_{it} + \beta_{it}), && i = 1, \cdots, m, \quad t = 1, \cdots, T \\
& \sum_{i=1}^{m} x_i^h + x_i^c = 1, \\
& x_i^h p_i^h - \alpha_{it} \geq 0, && i = 1, \cdots, m, \quad t = 1, \cdots, T \\
& x_i^c p_i^c - \beta_{it} \geq 0, && i = 1, \cdots, m, \quad t = 1, \cdots, T \\
& x_i^h \geq 0, \quad x_i^c \geq 0, && i = 1, \cdots, m, \\
& \alpha_{it},\ \beta_{it} \geq 0, && i = 1, \cdots, m, \quad t = 1, \cdots, T.
\end{aligned}$$

For simplicity of exposition, we can relax the finite distribution support of the random variables. Therefore, we have used $\tilde{z}_{it} = \tilde{v}_{it} - \tilde{w}_{it}$ where $\tilde{v}_{it} \geq 0$ and $\tilde{w}_{it} \geq 0$ for $i = 1, \cdots, m$ during the proof of this result as in Appendix B. Finally, it is worthwhile to note that since the error terms in the temperature model are independent from each other, we define the factors as the error terms for the computational study.

6. Design of Numerical Experiments and Data Analysis

This section is concerned with various implementation issues of the proposed models and data analysis. In particular, we focus on design of numerical experiments, data description, temperature modelling and estimation of model parameters. The computational results are presented and analysed in Section 7.

6.1. Design of Experiments

In order to illustrate performance of the stochastic and robust portfolio allocation models under temperature uncertainty, we conduct a series of numerical experiments using real data. Specifically, the computational experiments aim to answer the following questions:

- How does the investor's risk preferences affect the investment decisions using weather derivatives?
- How do the robust portfolio management models perform when the underlying temperature noise follows different distributions with symmetric and asymmetric characteristics?

- How do the model parameters such as the level of robustness affect the investor's decision on asset allocation and the portfolio wealth?

In order to answer these questions, we implement the single-period portfolio management problem and its corresponding robust formulations in MATLAB using the modelling interface YALMIP (Lofberg, (2004)) and the second-order cone programming solver GUROBI. We also use R for statistical analysis, in particular normality test with GH distribution.

Model Performance: The performance of the portfolio allocation models is measured in terms of optimal asset allocation, expected portfolio wealth and various risk measures. The robust optimization approach is benchmarked against traditional stochastic programming approach using expected value optimization and scenario-based optimization models since they are adopted in many practical applications. The single period stochastic portfolio management problem is formulated as an expected value optimization model (P_{nom}) in view of 1000 generated scenarios with equal probabilities. The robust portfolio allocation model (R_{nom}) is the robust counterpart of the nominal portfolio allocation (P_{nom}) and considers symmetric (R_{sym}), asymmetric (R_{asym}) and scenario based uncertainty sets with CVaR risk metric (P_{cvar}). In addition to the optimal investment strategies obtained by the traditional stochastic portfolio optimization approaches, we also consider a naive equally weighted investment strategy (abbreviated as "E-W (1/N))") as a benchmark to compare with performance of the robust portfolio optimization models. In this case, the optimal portfolio is constructed by weather futures contracts across all available locations. The CVaR investment strategies are tested at different percentiles since an investor may be concerned with extreme portfolio outcomes. Due to length limitations, we only present the results obtained by the CVaR optimization at 5% for illustrative purposes. We can report that both investment strategies - CVaR at 1% and 5% - at varying moments of error distributions behave in the same manner.

Simulation Experiments: We design simulation experiments to illustrate impact of model parameters and different error estimations of temperature uncertainty on the investment decisions. For each experiment, a sample of ten-thousand simulation paths (future realizations) of the random parameter is generated by predetermined distributions such as normal distribution, extreme value theory (EVT), generalized hyperbolic (GH), hyperbolic (HD) and t-distributions. Once the portfolio management models (robust or nominal) are solved to find an optimal investment strategy, we evaluate the optimal investment strategy using those simulated realizations of noise in the temperature model. Thus we obtain ten thousands of terminal wealth points evaluated by the optimal strategy on simulated temperature estimations. Finally, we statistically analyze the sample points evaluated with the optimal strategy. We summarize the results of statistical analysis in terms of average and variance of those evaluated simulations. We also compute value-at-risk (VaR) and conditional value-at-risk. The VaR at 5% is found by taking the 500th smallest value whereas the CVaR is calculated as an average of the 500 smallest values of all simulations. Due to length limitation we only present statistical analysis of simulated sample points in terms of average of terminal wealth (labelled as "Expected Wealth") and the CVaR (labelled as "Conditional Value at Risk 5%") with respect to varying moments of random distributions. We also report different characteristics of the portfolio selection models.

Sensitivity Analysis: In order to determine response of the portfolio optimization models to changes in the market conditions, the moments of random innovations (including mean, variance, skewness and kurtosis) are independently varied for the sensitivity analysis of temperature errors. In other words, a distribution is generated from the distribution of normalized random temperature errors ($\tilde{\varepsilon}$) having zero mean and unit

variance. For instance, for HDD temperature indices a positive shift over the mean of the temperature error process corresponds to a hotter temperature than the seasonal average value. Then we can test possible effect of a hotter season, which may decrease the value of HDD contracts during the winter period, on the investment decisions. Therefore, in order to change the mean error we add a constant amount to each randomly generated sample point. Similarly, when a distribution of random innovation ($\tilde{\varepsilon}$) is multiplied by a constant parameter c, then mean and volatility of $(c \cdot \tilde{\varepsilon})$ become zero and c, respectively, while its skewness and kurtosis remain the same. Therefore, we only change c in order to examine effect of varying volatility.

For testing effect of skewness of innovations on the optimal investment decisions, Chi-Square family of distributions is used as suggested by Chaffin and Rhiel (1993). Recall that a Chi-square distributed random variable $\tilde{\varepsilon}'$ with k degrees of freedom has mean k, variance $2k$ and skewness $\sqrt{8/k}$. Moreover, a linear transformation on the random variable does not affect its skewness. We generate a random variable with a positive skewness $\sqrt{8/k}$ using the linear transformation $(\tilde{\varepsilon}' - k)/\sqrt{(2k)}$. Similarly, a negatively skewed random variable corresponds to negative sign of the transformations.

We consider the contaminated normal family of distributions for testing leptokurtic distributions assuming that the underlying random error follows either a standard normal distribution $\mathcal{N}(0, 1)$ with probability p or a normal distribution $\mathcal{N}(0, S)$ with (variance S and) probability $1 - p$ (Chaffin and Rhiel (1993)). For sensitivity analysis regarding with varying kurtosis of temperature errors, we use $S = 4$ and vary p to achieve the desired level of kurtosis that is ranging between 3 and 8 to cover empirical values of historical temperature data. The corresponding probabilities are 0 and 0.73 for kurtosis levels at 3 and 8, respectively.

6.2. Data Description

We consider calendar-month futures contracts (traded in the CME) on temperature indices for empirical experiments. The weather derivatives are written on heating-degree-days and cooling-degree-days. We have gathered historical daily average temperatures from 24 locations in the United States and from 10 major locations in the United Kingdom. The daily average temperatures are measured on Celsius (UK) or Fahrenheit (USA) scale and computed as the average of the minimum and maximum temperature over the day. The US daily temperature data regarding with 24 locations from 1973 to 2013 is obtained from the National Climatic Data Center website. The UK temperature data for 10 locations is gathered from 1960 to 2006 by the Met Office, the UK's National Weather Service.

The descriptive statistics of daily mean temperatures for the US (Fahrenheit) and UK (Celsius) based locations are summarized in terms of average, variance, skewness, and kurtosis in Table 1 (Appendix A1). We observe that daily mean temperatures of cities in America display a wider spectrum (in range of $46.30°F$ and $69.26°F$) than mean temperatures of locations (in range of $8.87°C$ and $11.24°$C) in the UK due to geographical distance between locations. Apart from those positively skewed locations (namely Las Vegas, Los Angeles, Portland, Sacramento, Salt Lake City), the other locations in America and all locations in the UK possess negative skewness. However, both the US and UK locations have positive excess kurtosis.

6.3. Temperature Modelling and Validation

The temperature model described in Section 3 consists of deterministic (μ_{it}) and stochastic (δ_{it}) components and they need to be estimated from the historical data. For the deterministic part involving seasonal and cyclic components, we first estimate parameters $a_{0i}, a_{1i}, a_{2i}, a_{3i}$ of the seasonality function s_{it} for each

location i by regressing through time index over the past 40 years of data. The remaining part from the regression equation is then auto-regressed in order to estimate coefficients l_{1i}, l_{2i} and l_{3i}.

We present the estimated parameters of the temperature model in Table 2 (Appendix A2). Notice that all locations apart from Los Angeles have a positive trend component in the seasonality function. This can be interpreted as the effect of global warming that is at the highest level in Tuscon (2.29×10^{-4}) where the average temperature has risen by 3.42 $^{\circ}F$ during the last 41 years. In addition, the highest (the lowest) average difference between the hottest and the coldest days for Minneapolis (Los Angeles) is estimated as $61.04^{\circ}F$ ($16.40^{\circ}F$). The magnitude of seasonal squared volatility (ρ_{it}^2) is modelled by a cosine process and estimated by regressing the square of stochastic component with respect to time index. From the estimated parameters (b_0, b_2, b_3) of the seasonal volatility function, we observe that the variability of the volatility changes from a city to another and the highest variability in the volatility function is observed during the cold season (i.e. high values in column b_2 means high variability in the volatility function). For example, in Dallas the volatility increases up to 9.43 (2.76) during the winter (summer). This confirms the use of time dependent volatility for temperature modelling.

The remaining errors are computed from the division of the stochastic part by seasonal volatility and this leads to an error process with zero mean and unit variance. However, the errors for each location at the same time period are correlated to each other. Thus we model vectors of unit errors at each time period as factors equal to the number of locations multiplied by the dependence matrix σ. It is worthwhile to mention that QQ plots in Appendix A4 are based on independent factors related to each location and derived by multiplying the normalized residuals with the inverse of the dependance matrix. The covariance matrix (consisting of σ_{ij}) of the remaining residuals after removing the seasonality is computed via the Cholesky factorization method provided in Matlab. From the AR(3) process and time dependent volatility of residuals, we see that there exist highly correlated locations such as Baltimore and Washington D.C. (with correlation coefficient around 0.95). This obviously confirms the importance of the spatial model for the portfolio management problem using weather (temperature) products.

Residual Analysis: In order to validate the temperature model presented in Section 3, we analyse the historical average temperature data for each location. For illustrative purposes, we present the findings of data analysis of Atlanta in Appendix A4. Figure 1 (Appendix A4) displays the histogram and the autocorrelation function (ACF) for temperature observations. The temperature data shows non-normality and strong seasonality characteristics. We obtain the de-trended and deseasonalized temperature data by subtracting the seasonal component from each data point. Figure 2 (Appendix A4) presents the histogram, the autocorrelation function and the partial autocorrelation (PACF) for deseasonalized temperature observations in Atlanta. The PACF shows a strong evidence for autocorrelation of higher degrees than 1. This basically justifies the use of autoregressive function AR(3). On the other hand, degrees of AR higher than 3 lags become insignificant quite fast for the temperature data as reported by Saltyte-Benth and Benth (2012). The autocorrelation and the partial autocorrelation functions for the residuals after removing the autoregressive components are plotted in Figure 3 (Appendix A4). It is clearly seen that although AR(3) is acceptable to explain the autoregressive pattern, the seasonality in the volatility is still observed (by examining the autocorrelation function of the squared residuals).

For a validation of the temperature model, we also adopt an approach introduced by Saltyte-Benth and Benth (2012) using historical observations and one-step-ahead predictions of temperatures in the US

and UK locations. For each historical data points, the prediction of next-day temperature is computed via mean temperature defined in (1). The difference between the predicted temperature and the real (observed) temperature determines the prediction error (PE). The results of residual analysis for the estimated and predicted errors in terms of mean absolute error (MAE) and root mean squared error (RMSE) are summarised in Table 3 (Appendix A3). For error terms ϵ_{it} over periods $t = 1, \cdots, n$ at location i, $\text{MAE}(i) = \left(\sum_{t=1}^{n} |\epsilon_{it}|\right)/n$ and $\text{RMSE}(i) = \sqrt{\left(\sum_{t=1}^{n} \epsilon_{it}^2\right)/n}$. The prediction interval (PI) for the day-ahead temperatures is built through simulation of day-ahead temperatures and 95% and 99% PIs together with the percentage of predicted values outside of them are reported.

Normality Tests: Next, we proceed by regressing the error terms against the quantiles of a standard normal distribution. The residuals obtained from the regression analysis represent error rates in the temperature model and compare sample error data (on the vertical axis) to a standard normal population (on the horizontal axis). Normal QQ plots of daily error terms of Atlanta, Kansas City, Los Angeles and Portland (from left to right) against a normal reference distribution, presented at top panel of Figure 4 (Appendix A5), indicate the lack of fit to the regression line for some cities, and consequently, a departure from normality. The empirical quantile of the temperature error terms tends to be larger than the corresponding quantiles of a normal distribution. We also apply Kolmogorov-Smirnov test for normal distribution. The normality hypothesis for all locations apart from Liverpool, New York and Portland are rejected. The p values can get as low as 10^{-90} for Tuscon. This confirms that a normal distribution is a poor model to use. The S-shaped trend basically indicates that error distribution is skewed and displays fat-tails rather than a normal distribution. For the US cities, the skewness of the errors varies between -1.2418 (for Houston) and 0.2558 (for Los Angeles) while the temperature residuals associated with the UK locations are all negatively skewed. On the other hand, the residuals associated with all locations in both countries possess positive excess kurtosis. As a result of an extensive data analysis, we conclude that the temperature error distributions for both the US and UK locations are heavy tailed and for most of them the normality test fails.

In order to model skewed and fat-tailed structure of data sets, we consider Generalized Hyperbolic (GH), Hyperbolic (HD) and t-distribution to model temperature errors. In addition to this, we also take into account extreme cases of data set using Extreme Value Theory (EVT). For a detailed review on those distributions and their applications, the reader is referred to McNeil et al. (2005). The results of fitting temperature errors of EVT, GH, HD and t-distributions displayed in Figure 4 (panels 2, 3, 4, and 5, respectively, in Appendix A5) show that the EVT distribution is poor for explaining the residuals and GH distributions produce much better fits of temperature errors than the normal error distribution. As a result, we can say that the quantiles of GH distribution mostly fit the sample quantiles. For all computational experiments, we generate future temperature realisations by GH distribution.

6.4. Input Parameters to the Portfolio Allocation Models

There are specific parameters that are input to the portfolio allocation models and need to be either estimated from the historical data or generated via the temperature model (described in Section 3). In particular, the CVaR optimisation model requires a set of scenarios representing discrete realisations of the temperature uncertainty at each time point in the future. Notice that the future temperature scenarios are also to be generated for the sensitivity analysis of model parameters in simulations experiments. For generating scenarios in these experiments, we apply the same procedure whose brief description is as follows.

As the first step, a random vector of error terms (following a distribution with zero mean and unit variance) at each time period through the investment horizon is generated (as being factors equal to the number of locations). These vectors are used to create dependent error terms via the dependence matrix. The stochastic component for each period t is determined by multiplying dependent errors by seasonal volatility (ρ_{it}). The auto regressive component is then added (by multiplying the stochastic component of previous periods with the corresponding reversion values). As the final step, the seasonal temperature averages (s_{it}) are added. The resulting temperature process for given time horizon leads to a future temperature scenario. A set of scenarios can be generated in the same manner.

An important step of implementing the robust portfolio models is to determine uncertainty sets and inputs that make sense given available data. The inputs to the robust optimization models are the estimated moments of uncertain parameters and deviations of random factors. For the robust portfolio optimization models with symmetric uncertainty sets, we estimate expected values and covariance matrices of the temperature errors associated with locations under consideration using the historical data. In case of asymmetric uncertainty set, we calculate the forward and backward deviations for each random variable by following the procedure introduced by Natarajan et al. (2008). We construct an asymmetric distribution for temperature random variables at various levels of backward and forward deviations for the simulation based experiments. A two-variate asymmetric distribution for the simulated future temperature realizations is generated as $\varepsilon_i = \frac{\sqrt{\beta_i \cdot (1-\beta_i)}}{\beta_i}$, and $-\frac{\sqrt{\beta_i \cdot (1-\beta_i)}}{(1-\beta_i)}$ with probability β_i, and $1-\beta_i$, respectively. The resulting distribution of random parameter has zero mean and unit standard deviation as well as different levels of backward and forward deviations. In particular, if $\beta < 0.5$ ($\beta > 0.5$), then it has forward (backward) deviation equal to 1 whereas backward (forward) deviation is greater than 1. As $\beta < 0.5$, parameter gets closer to 0 (1) backward (forward) deviation increases.

The size of an uncertainty set is described by the price of robustness (corresponding to κ and Ω for the symmetric and asymmetric uncertainty sets, respectively). It is basically related to guarantees on the probability that the constraint involving uncertain coefficients will not be violated. For the computational experiments, we vary the value of price of robustness PoR_i within a specific range as an indicator of different risk averseness. It is arbitrarily generated as $PoR_{i+1} = PoR_i \times (1 + 0.5^{(i/7)}) + 0.05$ for $i = 1, 2, \cdots$ where $PoR_1 = 0$. This provides exponentially increasing values of price of robustness starting from 0.05. Moreover, from the numerical study we observe that the robust portfolios that are constructed by the budget of robustness higher than 2.76 consist of a weather derivative based on single location. Therefore, we only present the results of robust investment strategies obtained at price of robustness within $[0, 2.76]$ so that the optimal portfolio strategy is diversified among various weather contracts associated with different locations.

The other input parameters to the optimization models are selected as follows. The duration of weather contracts is one month. The tick size is \$20 for heating (p_i^h) and cooling (p_i^c) contracts based on location i. The financial data regarding with future prices of the underlying contracts is not publicly available. Therefore, the contractual prices $\bar{f}_i$ and $\bar{g}_i$ of weather derivatives associated with location i are generated by attaching a random factor (between 0.95 and 1.05) to the average HDD and CDD levels for the upcoming month. The randomness reflects the market related uncertainty or possible supply-demand imbalance.

7. Computational Results

In this section, we present the results of numerical experiments to illustrate performance of the portfolio allocation models and impact of uncertainty sets as well as model parameters on the optimal investment strategy and to analyze temperature risk management from the perspective of reducing estimation error on random temperature noise.

7.1. Performance of Portfolio Management Models

We are first concerned with performance comparison of various investment strategies (obtained by the stochastic and robust portfolio optimization models) in terms of optimal asset allocation of weather futures for HDD and CDD temperature indices on winter and summer periods, based on the US and UK locations.

Optimal Asset Allocation: Figure 1 illustrates optimal asset allocations obtained by solving the CVaR optimization model (left) at different targeted wealth and the robust portfolio management models under symmetric (middle) and asymmetric (right) uncertainty sets at varying price of robustness using HDD (top panel) and CDD (middle panel) indices for the US locations as well as HDD (bottom panel) indices for the UK locations. Different colours in Figure 1 represent asset allocations (weights) of various futures contracts on different locations. Note that the optimal asset allocation using the CDD temperature indices based on the UK locations is not presented in this figure since these contracts lead to a conservative strategy suggesting to invest on single location. Recall that, during the summer period, the worst-case temperature is below the threshold level (i.e. average temperature around 18^{o}C) in Britain.

For a fixed price of robustness, the optimal solution of the robust portfolio allocation models under symmetric and asymmetric uncertainty sets determines an investment strategy using weather derivatives on the worst-case temperature error estimation within the corresponding uncertainty set. For the price of robustness that is fixed at zero, the nominal model produces an optimal strategy that invests on single location with the highest return. Generally speaking, Figure 1 shows that the robust portfolios constructed by CDD (HDD) weather derivative contracts using symmetric and asymmetric uncertainty sets display different (same) characteristics. More precisely, we make the following observations:

- The robust decision-making models under symmetric and asymmetric uncertainty sets at fixed price of robustness within a range [0.05, 1.92] provide well-diversified portfolios of HDD weather derivative contracts among different locations in the USA. Note that the northern cities have mean temperature below the reference temperature during the winter period. For high price of robustness varying within [1.92, 2.76), the robust strategy (with both symmetric and asymmetric uncertainty sets) is still profitable and diversified. However, the robust model at fixed budget of robustness 2.76 suggests to invest on single location and provides zero profit at the worst-case. This implies that HDD weather derivative contract at the worst-case has no value at certain threshold of budget of robustness (i.e. any allocation gives 0 for the contract).
- The robust portfolios, constructed by the CDD weather derivative contracts based on several US locations, are profitable during August unlike those contracts based on the UK locations due to the climate. Note that during the summer the mean daily temperature at any location in the UK does not exceed 18°C. Thus, the worst-case temperature remains below the threshold level and the robust portfolio consists of a weather future for single location. For the CDD temperature indices based on

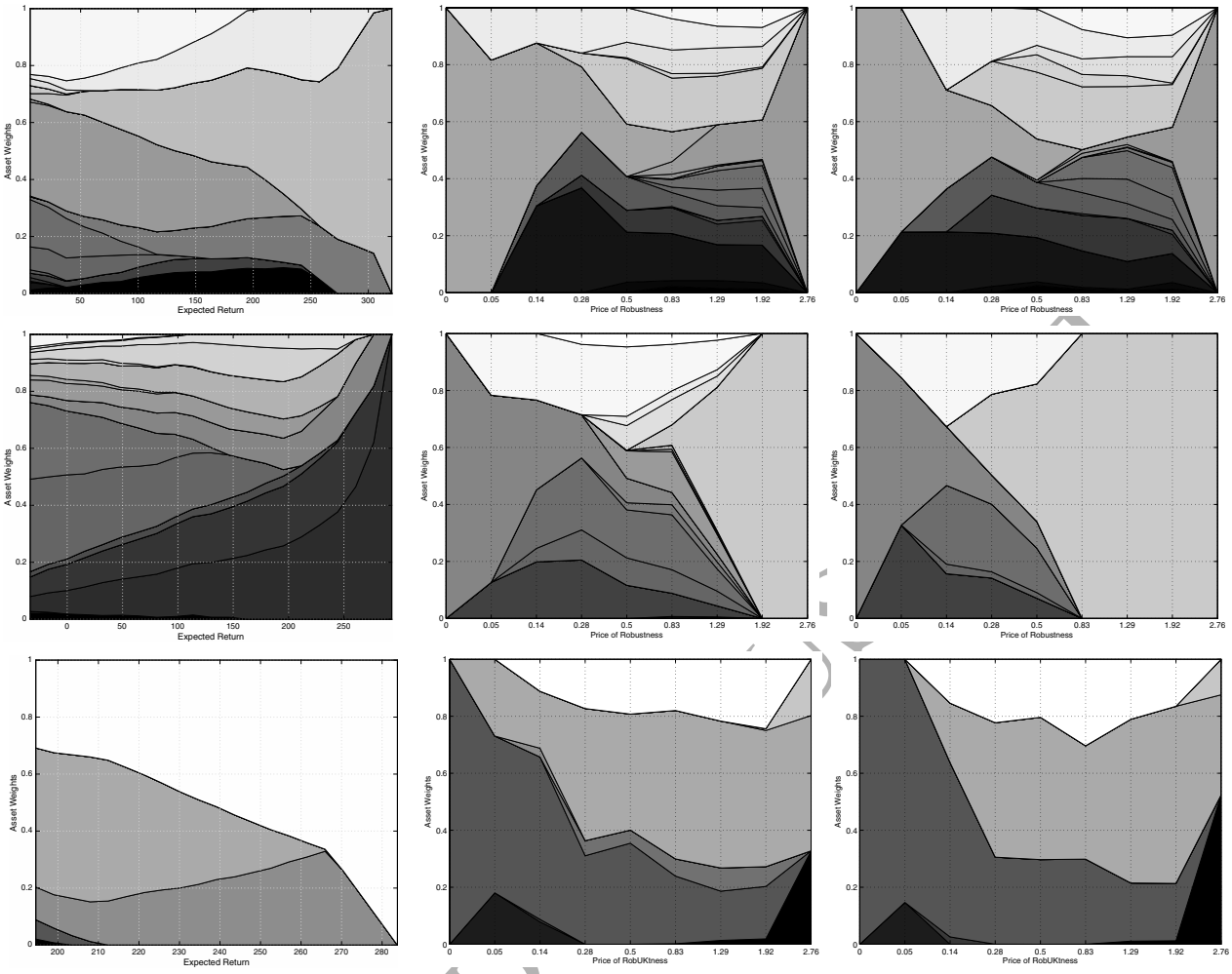

Figure 1: Optimal asset allocations obtained by the CVaR optimization model (left column), robust optimization with symmetric (middle column) and asymmetric (right column) uncertainty sets using HDD (top row) and CDD (middle row) weather derivatives for the US locations and HDD (bottom row) indices for the UK locations.

the US locations, the robust portfolios constructed using the symmetric (asymmetric) uncertainty set are diversified for the budget of robustness varying within [0.05, 1.92] ([0.05, 0.83]).

- The nominal strategy at zero price of robustness suggests to invest on HDD (CDD) contracts based on Minneapolis (Las Vegas) while the robust strategy with the highest price of robustness, at 2.76, considers HDD (CDD) contracts based on Los Angeles (Portland for symmetric and asymmetric uncertainty sets, respectively). For the UK data set, the nominal strategy also prefers single location of Edinburgh. However, the robust portfolio optimization model (at price of robustness 2.76) provides a well diversified asset allocation strategy among the HDDs based on London, Belfast and Cardiff.
- The CVaR investment strategies for both HDD and CDD temperature contracts of the US locations provide diversified portfolios consisting of different locations in America when the expected target return is low. As the target portfolio wealth increases, the investment strategies suggest to invest on single location: that is Philadelphia and Cincinnati for HDD and CDD contracts, respectively. A similar pattern is observed for HDD contracts based on the UK locations. The CVaR portfolios with targeted wealth in range [1210, 1265] consist of HDD temperature indices based on three locations

whereas the maximum wealth portfolio is constructed by only HDD contract of Southampton.

CVaR Investment Decisions: For performance comparison of the CVaR investment strategies obtained by weather futures written on HDD temperature indices for the US (left) and UK (right) locations, we construct the simulation-based efficient frontiers as follows. The lowest (W_{min}) and the highest (W_{max}) portfolio positions on the efficient frontier are obtained by solving the CVaR (5%) risk minimization problem (ignoring the portfolio wealth constraint) and the wealth maximization problem (ignoring the risk constraint), respectively. The range $[W_{min}, W_{max}]$ of minimum and maximum wealth portfolio positions is discretized by twenty points. At each discrete point on the frontier, we solve the CVaR minimization model (P_{cvar}) in view of the expected portfolio wealth constraint with fixed target-wealth $W_{target} \in (W_{min}, W_{max})$. As a result, the optimal asset allocations presented in Figure 1 (left column) are obtained. The optimal asset allocation at each discrete point is then evaluated with a sample of 10000 future temperature realizations generated by GH distribution with average errors 0, 0.05, and 0.1 (at fixed unit standard deviation) and standard deviations 0.5, 1, and 1.5 (at fixed zero mean). Figure 2 presents the simulation results in terms of average of the worst 500 evaluated paths in "Expected Wealth" and "Conditional Value at Risk 5%" space. We observe that the CVaR investment strategies produce the highest (lowest) expected wealth as well as

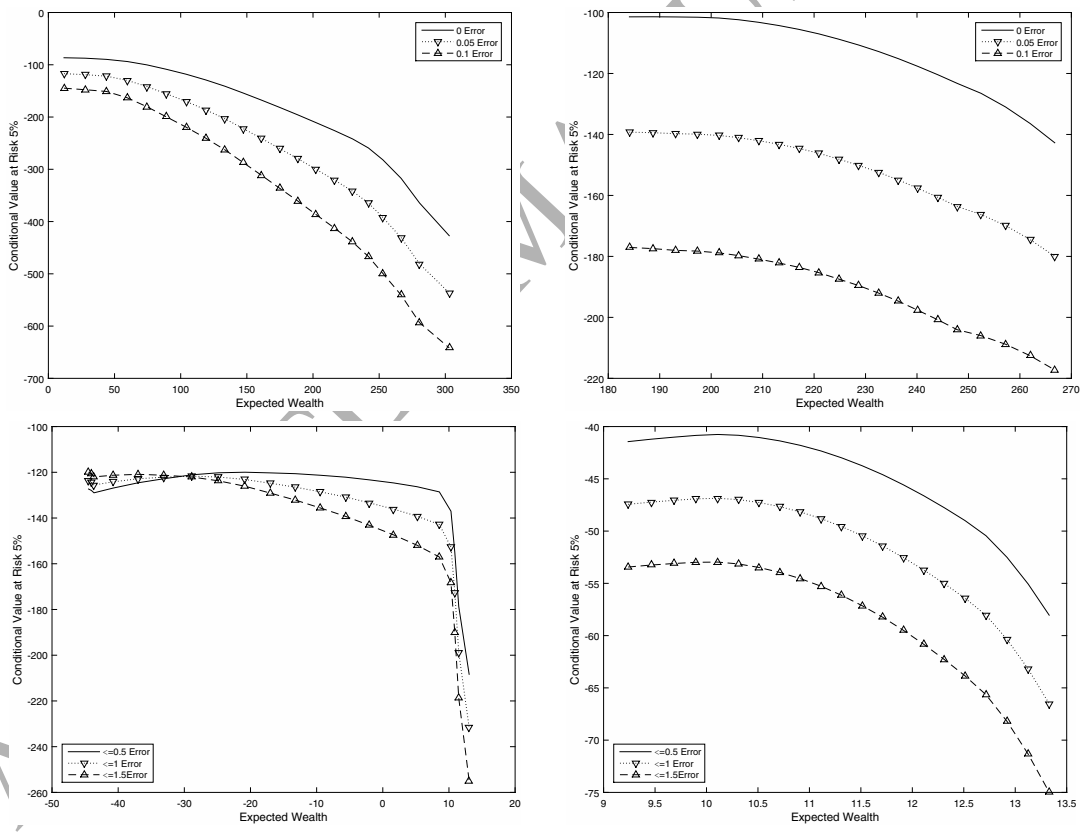

Figure 2: Impact of CVaR efficient portfolios using HDD temperature indices for the US (left) and UK (right) locations

the highest (lowest) "Conditional Value at Risk at 5%" when the future temperature realizations are distributed with low (high) mean (standard deviation, respectively). This performance can also be interpreted as analogue of a risk-return frontier relationship for the mean-variance portfolio allocation problem.

Performance of Robust Investment Strategies: In order to illustrate performance of the stochastic and robust portfolio allocation models as well as the naive equally weighted investment strategies, we design simulation experiments using two cases (labelled as "Case I" and "Case II"). In Case I, temperature realisations are generated by a skewed distribution with mean 1.4 at fixed unit standard deviation whereas Case II uses a skewed distribution of temperature realisations with zero mean and variance 1.9. It is worthwhile to emphasise that Cases I and II basically aim to create *unfavourable* and *favourable* weather conditions to express "*weather conditions that were different than expected on average*" and "*weather conditions as we expected*", respectively. Table 1 summarises the results of simulation experiments using investment strategies obtained by the stochastic portfolio allocation problem (nominal model, henceforth abbreviated as "N-M") and the robust optimization models under ellipsoidal uncertainty set (abbreviated as "R-S") at various budget of robustness (PoR). We also consider an equally weighted portfolio (abbreviated as "E-W $(1/N)$") that is constructed by $1/N$ asset allocations where N is number of temperature derivatives based on various locations under consideration.

Performance Statistics	HDD Indices Based on the US Locations						HDD Indices Based on the UK Locations					
	Mean	S-Dev	Skew	Kurt	VaR	CVaR	Mean	S-Dev	Skew	Kurt	VaR	CVaR
Models	*Case I: Skewed distribution with high-mean (1.4) and low-variance (1.0)*											
N-M (0)	67.10	72.03	-0.45	3.00	27.18	16.30	-46.80	116.09	-0.39	3.18	-71.95	-81.06
R-S (0.05)	71.47	65.34	-0.45	2.89	25.86	16.75	-52.42	131.36	-0.41	3.73	-79.45	-84.41
R-S (0.14)	64.26	35.56	-0.46	2.81	33.98	29.40	-50.98	124.65	-0.43	3.42	-73.60	-80.18
R-S (0.28)	66.49	28.43	-0.46	3.03	35.49	29.91	-48.33	120.08	-0.39	3.53	-69.21	-75.62
R-S (0.50)	68.52	20.85	-0.47	3.05	30.52	27.06	-48.57	120.66	-0.41	3.39	-70.35	-75.51
R-S (0.83)	71.76	18.56	-0.45	2.97	25.23	22.47	-47.27	119.90	-0.40	3.29	-69.85	-76.12
R-S (1.29)	77.97	15.15	-0.41	3.02	19.14	18.19	-47.80	118.68	-0.41	3.45	-68.10	-76.05
R-S (1.92)	89.47	15.45	-0.38	3.02	17.48	13.77	-46.96	118.78	-0.38	3.21	-70.90	-75.32
R-S (2.76)	82.95	14.08	-0.37	2.85	-16.88	-22.97	-52.32	129.94	-0.34	3.82	-75.40	-82.06
E-W(1/N)	69.60	14.52	-0.37	2.81	24.48	21.12	-45.86	111.65	-0.36	3.40	-67.75	-71.55
Models	*Case II: Skewed distribution with zero-mean and high-variance (1.9)*											
N-M (0)	201.70	94.97	-0.51	2.60	152.98	143.23	64.57	46.40	-0.41	2.79	30.51	23.70
R-S (0.05)	201.34	85.69	-0.53	3.03	155.05	145.79	63.21	25.31	-0.41	2.84	38.06	33.03
R-S (0.14)	170.63	50.05	-0.52	2.62	135.25	128.18	60.57	22.90	-0.40	3.19	36.64	31.85
R-S (0.28)	159.87	38.89	-0.54	2.98	128.68	122.45	57.66	21.68	-0.37	2.97	34.38	29.72
R-S (0.50)	144.80	29.20	-0.54	2.80	117.79	112.38	56.42	21.54	-0.38	3.36	33.21	28.57
R-S (0.83)	130.96	24.27	-0.50	2.79	106.33	101.40	54.82	21.53	-0.35	3.05	31.63	26.99
R-S (1.29)	119.86	21.97	-0.52	2.61	96.43	91.74	53.83	21.54	-0.34	3.05	30.63	25.99
R-S (1.92)	103.36	20.50	-0.50	2.72	80.73	76.20	53.09	21.55	-0.33	3.07	29.88	25.24
R-S (2.76)	92.21	18.32	-0.50	2.96	70.81	66.53	50.73	23.06	-0.32	2.73	26.72	21.92
E-W(1/N)	124.42	19.27	-0.51	2.80	102.08	95.32	53.73	20.25	-0.31	3.08	30.36	25.37

Table 1: Performance comparison of investment strategies with HDD indices based on the US (left) and UK (right) locations.

- In general, the optimal portfolios of HDD contracts regardless locations of the UK and America display a contracting behaviour in Cases I and II although they still keep specific characteristics of the underlying modelling approaches. We also observe an exceptional pattern in Case I using the HDD contracts based on the UK locations. In this case, all strategies produce negative wealth (loss) in average and the equally weighted strategy outperforms to the other strategies by achieving the lowest average loss and volatility. Recall that the distribution of future temperature realisations in Case II has higher volatility than the past observations while in Case I expectation of future forecasts is higher than the one observed from the past data.

- The nominal model (providing a risk-averse investment strategy) in Case II produces the highest wealth as well as the highest volatility in comparison with other strategies. However, when the investor has higher temperature expectation than the one observed in data (as in Case I), the nominal strategy of HDD contracts for the US locations provides one of the lowest wealth and the highest volatility. On the other hand, the performance of the equally weighted strategy takes place between performances of the robust and nominal models.
- Generally speaking, the robust optimization models based on the worst-case analysis behave differently in both cases. In Case II, robust portfolios of HDD contracts on locations of both America and the UK provide decreasing mean and standard deviation of portfolio wealth as the price of robustness increases. However, in Case I, as the price of robustness varies in range (0.05, 2.76), average portfolio wealth increases while the standard deviation of portfolio wealth decreases. This shows that expectation of forecasts plays an important role on performance of the robust investment strategies.
- In addition, from the results of robust portfolios of HDD on the US locations in Case I, we observe that the robust strategies at each price of robustness except 0.14 and 0.28 outperform (providing higher wealth than) the nominal strategy. Moreover, they persistently produce lower volatility when extreme (unfavourable) weather conditions are realised. Thus, we can say that when temperature forecasts have higher average temperature than the one estimated from the past data (as in Case I), robust portfolios of HDD contracts display a non-inferiority property that is referred as the worst-case performance.

The results in Table 1 clearly display that performance of weather investment strategies highly depend on the underlying model as well as the future temperature realizations. We exploit these observations further by carrying out an extensive empirical analysis.

7.2. Sensitivity Analysis

We conduct a sensitivity analysis in order to investigate impact of model parameters and characteristics of temperature distributions on investment strategies. More precisely, we aim to empirically establish possible effects of size and shape of uncertainty sets, choice of distributions of underlying random variable as well as moment estimations on performance of the portfolio allocation models using weather derivatives (HDD) based on the US and UK locations.

Choice of Uncertainty Sets: We first intend to analyse effect of the choice of uncertainty sets in portfolio management of weather derivatives by taking into account the investor's risk preferences. We consider discrete (scenario-based) and continuous (symmetric and asymmetric) uncertainty sets.

Scenario Based Uncertainty Set: A risk-averse investor wishes to minimize portfolio risk while achieving a pre-determined portfolio wealth. The minimum portfolio risk is obtained by solving the CVaR minimization model in view of 1000 temperature scenarios (see Section 4). The optimal asset allocation, obtained by solving the CVaR risk minimization model at fixed target portfolio wealth, is used for the simulation experiments. We select the target portfolio wealth as 1006, 1100, 1210 and 1320 (1194, 1221, 1252, and 1283) for weather derivatives based on locations in the US (UK). Notice that these four scenarios are chosen from the interval [1006, 1320] ([1194, 1283]) for the US (UK) locations (see Section 7.1). From the computational results, we find that an optimal strategy at fixed target wealth selected out of this range suggests to invest only one location. It is worthwhile to mention that the CVaR risk minimization strategy provides better diversification among different locations when the number of discrete scenarios is increased.

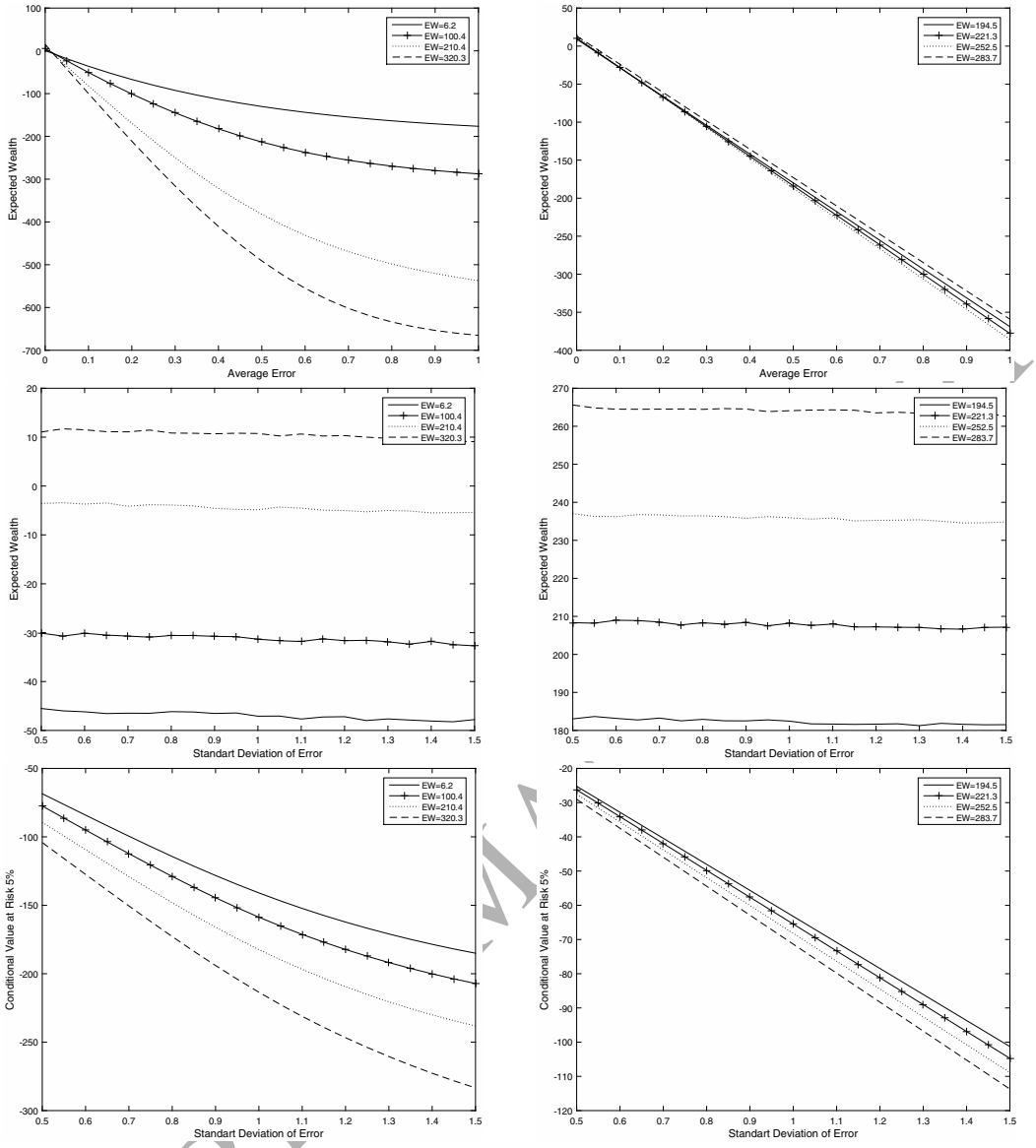

Figure 3: Performance of CVaR investment strategy using HDD temperature indices for the US (left) and UK (right) locations

The plots displayed in the first and second panels in Figure 3 summarize the simulation results obtained by varying mean temperature errors (at fixed unit standard deviation) and standard deviation of temperature errors (at fixed zero mean), respectively, for locations in the US (left) and the UK (right) in terms of mean wealth. The plots in the last panel present the simulation results in terms of average of the worst 500 evaluated paths at different standard deviation of temperature errors.

From results of the US case, we can easily observe that the optimal investment strategy that minimizes CVaR risk measure at the highest (lowest) target portfolio level provides the highest losses (lowest expected wealth) whereas the lowest target portfolio provides the lowest loss (highest expected wealth). As mean error of future temperature distribution increases, we obtain the worst-case loss by implementing an investment strategy obtained at the highest target portfolio level increases regardless the choice of data sets. For the UK case, however, performance of portfolios at the lowest and highest target wealth is very close in terms of

expected wealth. On the other hand, the estimated noise distribution with zero mean and standard deviation varying between 0.5 and 1.5 for the US and UK locations does not change the pattern of losses achieved by various investment strategies under temperature scenario uncertainty set. When the investor increases the portfolio target level (W_{target}), then the CVaR optimal strategy persistently provides high expected wealth and low conditional value-at-risk 5% at varying standard deviation of future temperature realizations.

Overall, these results confirm that a low targeted investment strategy performs better (worse) when the average (standard deviation) of temperature errors increases. We can conclude that when investor's CVaR risk preferences is considered, the choice of target portfolio position combined with the moments of noise distribution for future temperature realizations plays an important role on the weather risk management.

Symmetric and Asymmetric Uncertainty Sets: In order to understand impact of uncertainty sets and their shapes on the robust strategies, we design empirical experiments where future temperature paths follow different distributions as described in Table 2. Exp 1 considers a normally distributed (0.2 mean and unit

Experiment ID	Type of Distribution	Description
Exp 1	Symmetric	normal distribution, $N(0.2, 1)$
Exp 2	Asymmetric	historical positive deviations
Exp 3	Asymmetric	historical negative deviations
Exp 4	Asymmetric	random deviations
Exp 5	Asymmetric	fixed positive deviations
Exp 6	Asymmetric	fixed negative deviations

Table 2: Distributions of temperature noise

variance) temperature noise. For other experiments, we assume that future temperature realizations follow an asymmetric distribution with different forward and backward deviations. More specifically, Exp 2 and Exp 3 use positive and negative deviations as estimated from the corresponding historical data set, respectively. In Exp 5 and Exp 6, positive and negative deviations, respectively, are fixed for each location as 2. Exp 4 uses a random asymmetric structure where β_i for each location i is randomly selected from interval [1, 2]. The forward and backward deviations of an asymmetric uncertainty set (using $\beta_i < 0.5$) are specified (in experiments 2, 3, 4, 5 and 6) as follows. The case of *"historical"* asymmetric uses actual deviations estimated from the historical temperature data. For *"equal"* case, the forward and backward deviations are assumed to be constant and fixed as 2. For *"increasing"* and *"decreasing"* cases, an increasing and decreasing order of forward and backward deviations arising within interval [1, 3.4] are considered. *"Random"* deviations at each location do not follow any structure, but are randomly generated. Figure 4 illustrates performance comparisons of the robust models under symmetric and asymmetric uncertainty sets with fixed price of robustness at 1.3 (left) and 0.45 (right) using the US (top) and UK (bottom) locations for each experiment.

- As expected from Exp 1, the robust investment strategy under the symmetric uncertainty set provides higher wealth than the strategy under the asymmetric uncertainty set for both US and UK data sets regardless the choice of price of robustness since temperature forecasts follow a symmetric distribution. Similarly, as in Exp 2, $\cdots$, and Exp 6, the asymmetric uncertainty set with different shape of distributions (selecting different forward and backward deviations) outperforms the symmetric uncertainty set. This is due to the nature of future realizations having asymmetric characteristics.
- We also observe that the choice of deviations describing a shape of the asymmetric uncertainty has

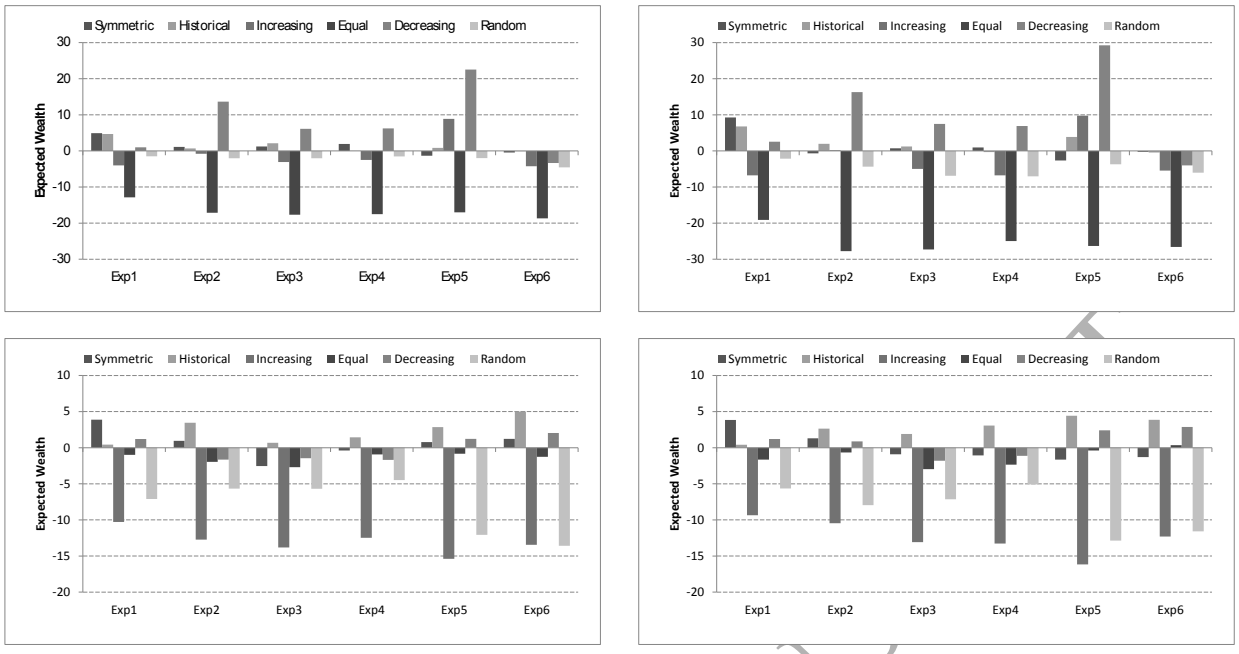

Figure 4: Performance comparisons of symmetric and asymmetric uncertainty sets at fixed price of robustness at 1.3 (left) and 0.45 (right) using the US (top) and UK (bottom) locations

an impact on the robust strategy. Furthermore, asymmetric structure follows the same pattern under different price of robustness. Decreasing (equal) asymmetric distribution produces higher (lower) expected wealth than other distributions using temperature indices based on the US locations. However, historical (increasing) asymmetric distribution using the temperature indices based on the UK locations provides the highest (lowest) wealth. An asymmetric uncertainty set with fixed deviations using both data sets behaves in more conservative fashion and, therefore, leads to the lowest wealth.

As a conclusion, we can say that distribution of various temperature realizations combined with the choice of uncertainty set plays an important role on the performance of the robust investment strategies.

Temperature Error Distributions: We now wish to investigate effect of various temperature error distributions on the optimal asset allocation. For this experiment, we evaluate the optimal investment strategy (obtained by solving the nominal and robust portfolio models for fixed price of robustness at 1.29) with each simulated future temperature index. A sample of future realizations of temperature indices is generated by various distributions with the same mean and standard deviation of temperature noise. Figure 5 displays the results of simulation experiments in terms of expected portfolio wealth for varying values of average errors (top panel) and standard deviation of noise (bottom panel).

The EVT distribution provides the lowest worst-case expected wealth of simulated temperatures while other distributions show the same decreasing performance pattern as average error of future temperature realizations increases. On the other hand, for standard deviation of future temperature realizations varying between 0.5 and 1.5 (fixed zero mean), all distributions except EVT provide increasing expected wealth of robust portfolios. In case of EVT, the investment strategies based on the US and UK locations produce the same decreasing pattern since EVT considers only extreme temperature cases. While t-distribution provides the best portfolio performance using HDD temperature indices based on the US locations, GH distribution

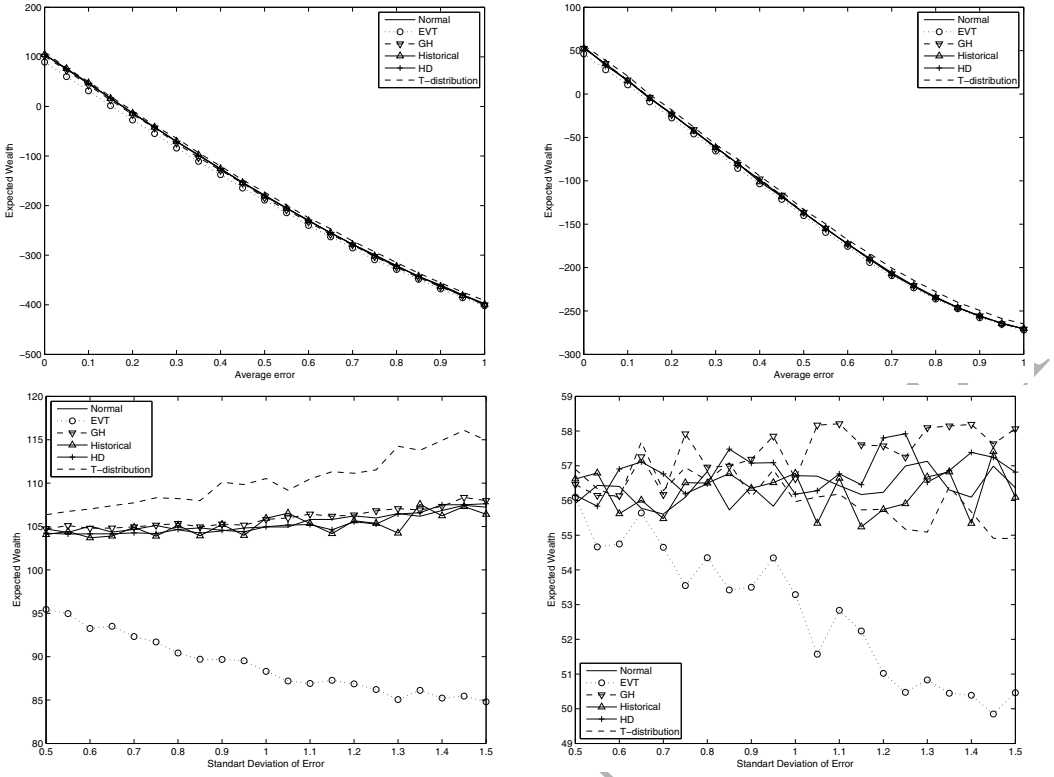

Figure 5: Impact of various temperature error distributions using the US (left) and UK (right) locations

outperforms for the UK case. Finally, a non-smooth behaviour of expected wealth of the portfolios using the UK locations (unlike in the US case) is observed at any level of standard deviation of temperature errors using any distribution. As a result, we can conclude that standard deviation (average) of temperature error distributions, used for generating future temperature realizations, has high (almost no) impact on the performance of robust strategies regardless locations of the weather derivatives.

Next we would like to establish how the moments of innovations might have impact on the optimal investment decision-making. We consider generalized hyperbolic distribution to generate future scenarios of temperature since it has been established by the data analysis as the best fit of the historical data.

Moments of Temperature Distributions: For this experiment, we conduct simulation experiments where the optimal strategies obtained from the nominal (with zero price of robustness) and robust portfolio allocation models (with fixed price of robustness at 0.14, 1.3, and 2.8) are evaluated with the simulated temperature errors of HDD weather contracts based on the US and UK locations. We compute statistical properties of simulation paths, but only present simulation results in terms of "Expected Wealth" and "Conditional Value-at-Risk at 5%" in Figures 6, 7, and 8. In Figure 6, the average temperature errors vary between zero and one (with fixed unit standard deviation) whereas standard deviation of temperature errors ranges from 0.5 to 1.5 (with fixed zero mean) in Figure 7. We also investigate performance of portfolio allocation models by varying higher order moments (skewness and kurtosis) of temperature errors using weather contracts based on the UK and US locations. From the computational results, we observe that skewness and kurtosis of error distributions seem to display the same performance characteristics in terms of impact on the investment decisions. Therefore, we only present the results of skewness for changing values

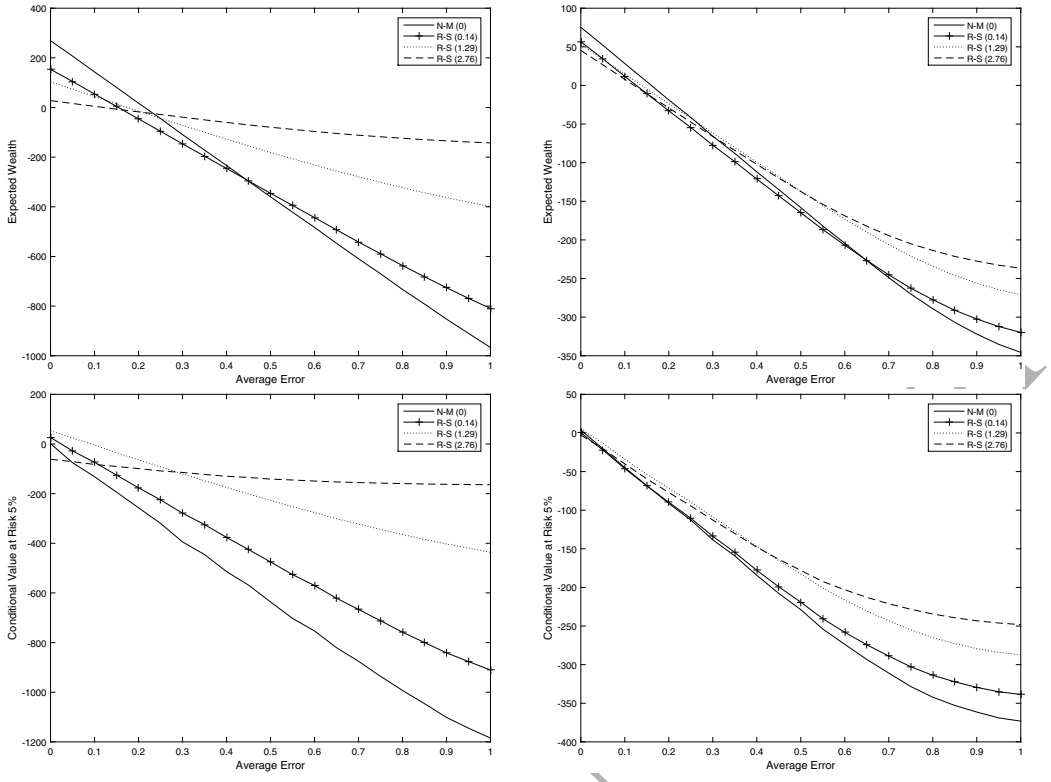

Figure 6: Performance of investment strategies for the US (left) and UK (right) locations at various average temperature errors

within [-1.5, 1.5] in Figure 8.

We can make the following observations from the results in Figure 6:

- An investor's expected terminal wealth depends on average, but not necessarily standard deviation, of temperature errors used for distribution of future realizations. For low average temperature errors (varying between 0 and 0.2 (0.1) for the US (UK) locations), the robust portfolio models (at price of robustness 0.14, 1.3 and 2.8) as well as the nominal portfolio model (at zero price of robustness) provide positive expected terminal wealth. In these cases, the nominal model outperforms the robust models. We also observe that the robust models with low price of robustness produce higher expected wealth than the ones with high price of robustness (described as more conservative models).
- As average temperature error increases (from 0.2 (0.1) to 1 for the US (UK) locations), the terminal wealth achieved by each portfolio becomes negative since the value of HDD temperature indices decreases (i.e. return of future weather derivatives decreases). At those error terms, the robust strategy with the highest price of robustness (2.8) provides the highest terminal wealth. In other words, the robust investment strategy allows the investor to be guarded against the worst-case. On the other hand, the nominal strategy produces the lowest wealth at unit average error.
- It is also worthwhile to mention that the gap between losses supplied by the robust models due to an investment on HDD derivatives for the US locations dramatically decreases as the price of robustness increases from 0.14 to 2.8. A similar pattern can be seen from the UK locations only for average temperature errors within interval [0.6, 1] where the gap is much smaller than the US case.

As illustrated in top panel of Figure 7, the standard deviation (varying between 0.5 and 1.5) of future

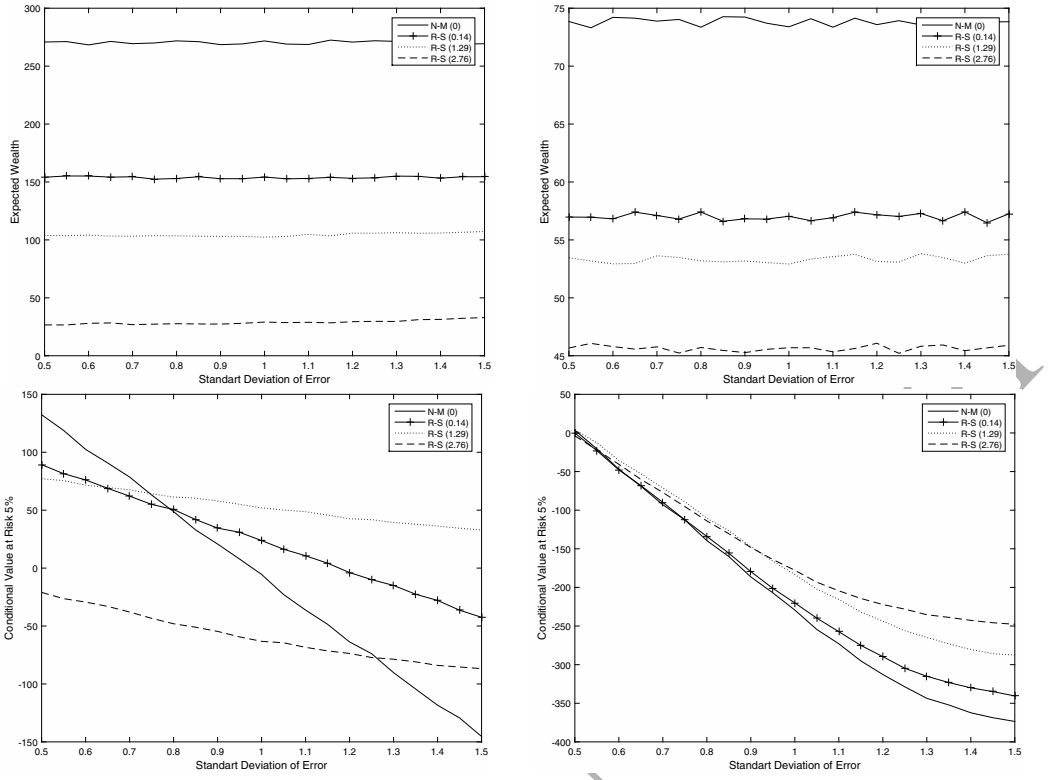

Figure 7: Performance of investment strategies for the US (left) and UK (right) locations at various standard deviation of temperature errors

temperature error realizations does not have impact on the performance of investment strategies as far as the expected terminal wealth is concerned. For both data sets, the nominal strategy persistently outperforms the robust strategy and it provides the highest expected terminal wealth when average of sample for future realizations of temperature errors is fixed at zero. As the price of robustness increases from zero to 2.8, the expected portfolio wealth decreases. However, each strategy remains stable for the US locations when the standard deviation of simulations increases. On the other hand, small variations for the UK data is realized, but the performance order of investment strategies remains the same.

We also observe that mean and standard deviation of temperature errors' distributions have impact on "Conditional Value at Risk 5%" for HDD contracts on locations of the US and UK. More precisely, values of CVaR 5% (loss) for all investment strategies decrease as mean (standard deviation of) error distributions vary from 0 to 1 (from 0.5 to 1.5) as shown (bottom panel) in Figures 6 and 7.

As can be seen from Figure 8, skewness of future temperature errors and expected portfolio wealth is negatively related. In other words, an increasing value of skewness decreases expected portfolio wealth obtained by all strategies regardless the type of HDD indices based on the US and UK locations while the performance order of all strategies remains the same starting from the nominal strategy (at the highest level) through the robust strategies at increasing price of robustness (at the lowest level). In terms of CVaR 5% of portfolio wealth, a general performance pattern is not seen.

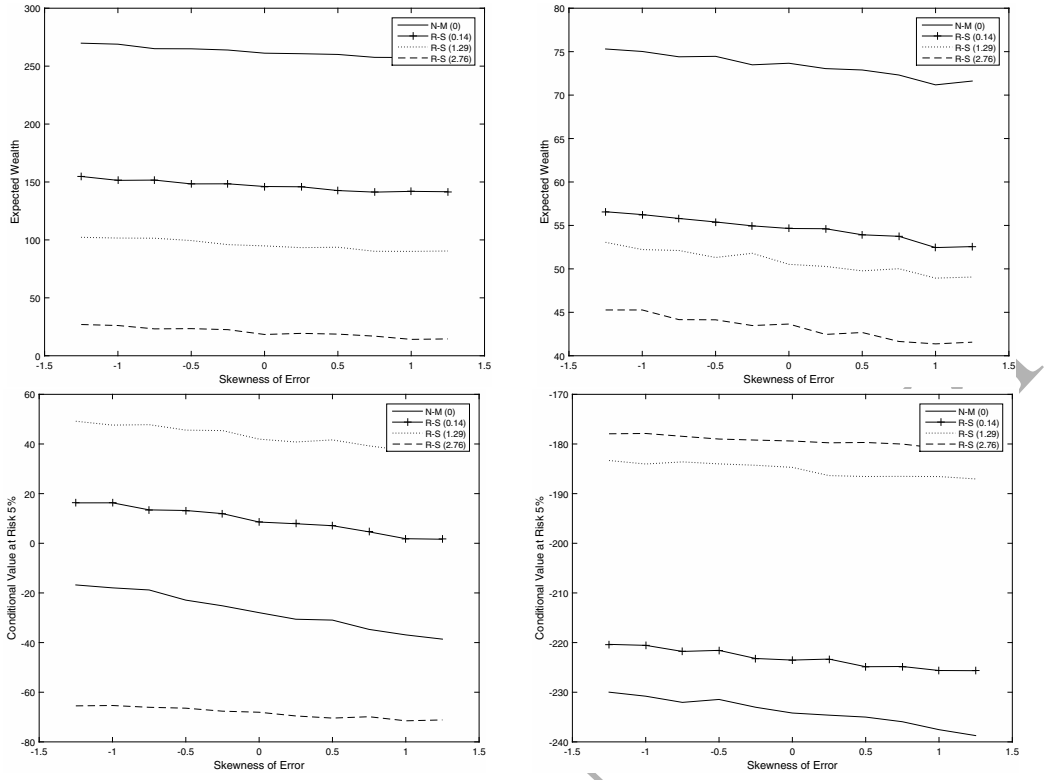

Figure 8: Performance of investment strategies for the US (left) and UK (right) locations at various skewness of temperature errors

7.3. Annualized Portfolio Performance and Risk Metrics

We also investigate economical performance of trading strategies based on monthly weather derivatives in terms of annualized return and risk-adjusted performance measures such as annualized volatility, Sharpe ratio, maximum drawdown and information ratio. The reader is referred to Bacon (2008) for further information on different portfolio measurements. A rolling horizon approach is adopted for one year investment horizon ($T = 12$) starting from the 1st of January. A myopic multi-period portfolio model is created as follows. At the beginning of each time period $t = 1, \cdots, T$, the corresponding portfolio optimization model is solved to determine the optimal asset allocation decisions for a month ahead. The portfolio wealth is computed at the end of time period t using the predicted future temperature. Then the amount of capital, that is gained in time t, is to be invested for time $t + 1$. We resolve the optimization problem to determine the derivative positions in time $t + 1$. This procedure is carried out till the end of investment horizon T. Since the duration of weather derivatives is for one month, it is not possible to keep the position of a given contract. We assume that the transaction cost for any of strategy (where the whole capital is invested to take a market position) remains the same over the investment horizon and not included for the numerical experiments. In order to eliminate possible effect of future temperature realisations, these experiments are repeated by 1000 different simulations. The average performance of portfolio return and risk metrics are computed over all simulations and these results are presented in Table 3.

The cumulative annual return is measured as average monthly portfolio return whereas the annualised volatility represents the variability of monthly portfolio return over a year. The Sharpe ratio defines a risk-adjusted portfolio return and is computed as the ratio of the excess return of the portfolio to its volatility

where the risk-free return is assumed to be 1%. As expected, the nominal strategy provides the highest annualized portfolio return and annualized portfolio volatility in average. On the other hand, as price of robustness increases, the robust strategies provide a decreasing annualised portfolio return as well as portfolio volatility, but an increasing Sharpe Ratio. The equally weighted portfolio's annualised return (3.40) and volatility (3.23) are higher (lower) than those values obtained by the robust strategy at price of robustness in range [0.83,2.8] ([0,0.83), respectively).

In Average Models (PoR)	Cumulative Annual Return	Annualized Volatility	Sharpe Ratio	Maximum Drawdown	Information Ratio
N-M (0)	7.47	9.60	0.737	6.93	0.412
R-S (0.05)	6.96	8.90	0.730	6.43	0.439
R-S (0.14)	6.18	7.26	0.789	5.99	0.703
R-S (0.28)	5.22	5.44	0.807	4.97	0.870
R-S (0.50)	4.23	4.21	0.817	4.19	0.459
R-S (0.83)	3.25	2.96	0.821	3.06	-0.128
R-S (1.29)	2.31	1.51	0.946	2.30	-0.503
R-S (1.92)	2.20	1.45	0.957	2.01	-0.491
R-S (2.76)	2.06	1.21	0.986	1.90	-0.435
E-W(1/N)	3.40	3.23	0.837	2.97	0.0

Table 3: Average annualised portfolio performance and risk metrics

Similarly, maximum drawdown expresses a type of downside risk over an investment period of a year. It represents the maximum loss from a peak to a trough of a portfolio, before a new peak level is reached. As Table 3 illustrates, the robust strategies at each price of robustness outperform (i.e. producing lower maximum drawdown than) the nominal strategy. In addition, the robust portfolios at price of robustness varying in (0.83,2.76] also provide lower maximum drawdown than the equally weighted portfolio does. Notice that the nominal strategy produces the highest maximum drawdown.

In order to compute the information ratio of the nominal and robust portfolios, the equally weighted portfolio is selected as a benchmark. The information ratio of a specific portfolio is expressed as the ratio of excess returns (difference between the portfolio returns and the benchmark portfolio returns) to the tracking errors (volatility of those excess returns). From Table 3, one can observe that the portfolios obtained by the robust strategy with low (high) price of robustness within range [0.05, 0.50] (and [0.83,2.76], respectively) provide higher (lower) information ratio than the portfolio of nominal strategy. A high information ratio highlights more consistency in terms of outperformance of the robust strategy with respect to the benchmark.

Finally, we conduct out-of-sample experiments to backtest performance of the different investment strategies using the HDD indices based on the US locations over a five-year investment horizon (that is monthly historical data from 2009 to 2013). The initial wealth is $1000. For this experiment, we first solve the portfolio problem at the beginning of a month and evaluate the optimal investment strategy for the next month to compute the portfolio wealth. Then for the upcoming months we rerun the portfolio allocation model with the updated wealth. By moving one month time window over the five-year investment horizon, we compute the final wealth (or cumulative portfolio profit) for each calendar month.

Figure 9 presents backtesting results in terms of portfolio wealth obtained by the nominal, robust (with a symmetric uncertainty set at different robust of budget) and equally weighted investment strategies. These results confirm that the nominal model (with no consideration of uncertainty) outperforms to other strategies whereas the equally weighted portfolio provides a similar performance as the robust strategy R-S (1.3). The

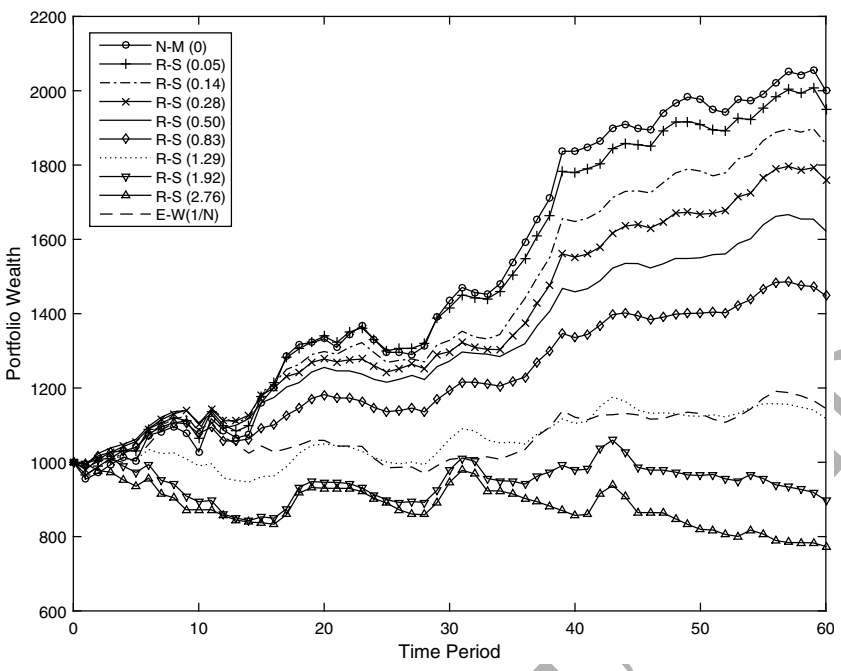

Figure 9: Backtesting results for HDD temperature indices based on the US locations

robust strategies at price of robustness varying from 0.05 to 1.3 produce lower portfolio wealth, but seem to be less volatile than the nominal strategy over the investment horizon. On the other hand, the most conservative robust investment strategies R-S (1.9) and R-S (2.8) produce the lowest portfolio wealth over the investment horizon (with decreasing performance pattern). Notice that the nominal strategy as well as the robust strategies with high price of robustness show a highly volatile behaviour over time.

8. Conclusions

In this paper, we study a single-period portfolio allocation problem under temperature uncertainty. We introduce a robust optimization approach for the portfolio allocation problem from the perspective of an investor who is dealing with temperature error distribution, and wishes to be protected against the worst-case realizations of the uncertain weather. We suggest a spatial temperature modelling where correlation between locations of weather derivatives under consideration is explicitly taken into account. This model can also be used for hedging purposes to obtain an insurance portfolio in practice.

Weather derivatives are traded on different locations for the purpose of insurance over various weather events. In this paper, the robust portfolio optimization approaches are proposed for weather derivatives to immunize an investment strategy against the uncertainty due to temperature forecasts. Although robust optimisation involves modelling and solving advantages in terms of, for instance, computational tractability for real life applications, it has some drawbacks. One of the limitations is the question of how to construct an uncertainty set and what size of the uncertainty set to choose. This drawback is extensively studied in computational experiments. We approximate the support of uncertain temperature error parameters in different ways by using specific shapes for the uncertainty sets. In other words, portfolio risk is integrated via robust optimization with symmetric and asymmetric uncertainty sets as well as a scenario uncertainty

set with the Conditional Value-at-Risk measure. The advantage of incorporating uncertainty through the uncertainty sets is that one does not need to make restrictive assumptions on the underlying dynamics of the processes for these uncertainties and can incorporate varying degrees of knowledge about the underlying random probability distribution.

From the extensive computational experiments, we can conclude that the robust portfolios provide better worst-case performance and produce a better diversification in comparison with the nominal model. The empirical study indicates that an investor's risk preferences, the choice of uncertainty set in view of different characteristics as well as price of robustness play an important role on the performance of the robust investment strategy. In particular, the sensitivity analysis on model parameters indicates that the investor's expected terminal wealth is highly affected by average, but not necessarily standard deviation or higher order moments of distribution of forecasts.

For better performance, the choice of an uncertainty set should best represent the characteristics of the probability distributions of future uncertainties. Data-driven approaches could be introduced for portfolio and risk management of weather derivatives. In this case, the uncertainty sets are constructed with certain structures and sizes that accord with the data. In addition, the portfolio allocation problem of weather derivatives can be modelled in a multi-period setting where a dynamic trading strategy can be imposed by introducing time dependent wealth as a state variable. Such a modelling approach suffers from the curse of dimensionality and may involve a problem structure with uncertain data arising in cross constraints that may lead a conservative strategy.

References

[1] Alaton, P., Djehiche, B., Stillberger, D., On modelling and pricing weather derivatives, Applied Mathematical Finance, 2002, 9 (1), 1–20.

[2] Bacon, C.R., Practical Portfolio Performance Measurement and Attribution, 2nd Edition, 2008.

[3] Bank, M., Wiesner, R., Determinants of weather derivatives usage in the Austrian winter tourism industry, Tourism Management, 2011, 32(1), 62–68.

[4] Barth, A., F.E. Benth, Potthoff, J., Hedging of spatial temperature risk with market-traded futures Applied Mathematical Finance, 2011, 18(2), 93–117

[5] Benth, F.E., Saltyte-Benth, J., Stochastic modelling of temperature variations with a view towards weather derivatives, Applied Mathematical Finance, 2005, 12, 53–85.

[6] Benth, F.E., Saltyte-Benth, J., The volatility of temperature and pricing of weather derivatives. Quantitative Finance, 2007, 7(5), 553–561.

[7] Benth, F. E., Saltyte-Benth, J., Koekebakker, S., 2008. Stochastic Modelling of Electricity and Related Markets. World Sci.

[8] Benth, F.E., Saltyte-Benth, J., Weather derivatives and stochastic modelling of temperature, International Journal of Stochastic Analysis, 2011, 1–21.

[9] Ben-Tal, A., L. El Ghaoui, A. Nemirovski, 2009, *Robust Optimization*, Princeton University Press.

[10] Ben-Tal, A., Nemirovski, A., Robust convex optimization, Mathematics of Operations Research, 1998, 23(4), 769–805.

[11] Bertsimas, D., D. Pachamanova, M. Sim, Robust linear optimization under general norms, OR Letters, 2004, 32, 510–516.

[12] Bertrand, J., X. Brusset, M. Fortin, Assessing and hedging the cost of unseasonal weather: case of the apparel sector, European Journal of Operational Research, 244(1), 2015, 261–276.

[13] Bertsimas, D., V. Gupta, N. Kallus, Data-Driven Robust Optimization, Submitted to Operations Research (2013).

[14] Brockett, P.L., M. Wang, C. C. Yang, H. Zou, Portfolio effects and valuation of weather derivatives, Financial Review, 2006, 41(1), 55–76.

[15] Brockett, P.L., Wang, M., Yang, C., Weather derivatives and weather risk management, Risk Management and Insurance Review, 2005, 8(1), 127–140.

[16] Brody, D.C., Syroka, J., Zervos, M., Dynamical pricing of weather derivatives, Quantitative Finance, 2002, 2(3), 189–198.

[17] Cao, M., Li, A., Wei, J., Watching the weather report, Canadian Investment Review, 2004, 27–33.

[18] Cao, M., Wei, J., Weather derivatives valuation and market price of weather risk, J. of Futures Markets, 2004, 24(11), 1065–1089.

[19] Chen, X., M. Sim, P. Sun, A robust optimization perspective on stochastic programming, Operations Research, 2007, 55(6), 1058–1071.

[20] Ceria, S., Stubbs, R., 2006, Incorporating estimation errors into portfolio selection: robust portfolio construction, Journal of Asset Management, 2006, 7(2), 109–127

[21] Dorfleitner, G., Wimmer, M., The pricing of temperature futures at the Chicago Mercantile Exchange, Journal of Banking and Finance, 2010, 34(6), 1360–1370.

[22] Elias, R.S., Wahab, M.I.M., Fang, L., A comparison of regime-switching temperature modeling approaches for applications in weather derivatives, European Journal of Operational Research, 232(3), 2014, 232, 549–560.

[23] Ellithorpe, G., Punman, S., Weather derivatives and their implications for power markets, The Journal of Risk Finance, 2000, 1(2), 19–28.

[24] El Ghaoui, L., Lebret, H., Robust solutions to least-squares problems with uncertain data, SIAM Journal Matrix Analysis and Applications, 1997, 18(4), 1035–1064.

[25] Fabozzi, F., Kolm, P., Pachamanova, D., Focardi, S., Robust Portfolio Optimization & Management, 2007, Wiley & Sons.

[26] Garman, M., Blanco, C., Erickson, R., Weather derivatives: instruments and pricing issues, Financial Engineering Associates, 2000.

[27] Goldfarb, D., G. Iyengar, Robust portfolio selection problem, Mathematics of Operations Research, 2003, 28(1), 1–37.

[28] Gorissen, B. L., Yanikoglu, I., Den Hertog, D., Hints for practical robust optimization, CentER, 2013, Vol. 2013–065.

[29] Gulpinar, N., Rustem, B., 2007, Optimal decisions and robust methods for forecast errors, Computational Statistics and Data Analysis, 2007, 51, 3595–3611.

[30] Hardle, K. W., Lopez-Cabrera, B., Ritter, M., Forecast based pricing of weather derivatives, 2012, SFB 649, 2012-027.

[31] Hamisultane, H., Utility-based pricing of weather derivatives, The European Journal of Finance, 2010, 16(6), 503–525.

[32] Jewson, S., Weather derivative pricing and risk management: volatility and value at risk, 2002.

[33] Jewson, S., Brix, A., Weather derivative valuation: the meteorological, statistical, financial and mathematical foundations, Cambridge University Press, 2005.

[34] Jewson, S., Weather derivative pricing and the potential accuracy of daily temperature modelling, Risk Management Solutions, 2004, London, UK.

[35] Kawas, B., Thiele, A., A log Â-robust optimization approach to portfolio management, OR Spectrum, 2009.

[36] Lofberg, J., YALMIP: A Toolbox for Modeling and Optimization in MATLAB. In Proc. of CACSD Conf., Taiwan, 2004.

[37] McNeil, AJ, Frey, R., Embrechts, P., Quantitative Risk Management: Concepts, Techniques and Tools, 2005, Princeton University Press.

[38] Musshoff, O., Hirschauer, N., Odening, M., Portfolio effects and the willingness to pay for weather insurances, Agricultural Finance Review, 2008, 68(1), 83–97.

[39] Moon, Y., Yao, T., A simple robust mean absolute deviation model for portfolio optimization, Computers and Operational Research, 2011, 38(9), 1251–1258.

[40] Natarajan, K., D. Pachamanova, M. Sim, Incorporating asymmetric distributional information in robust Value-at-Risk optimization, Management Science, 2008, 54(3), 573–585

[41] Rockafellar, R.T., Uryasev, S., Optimization of Conditional Value-at-Risk, The Journal of Risk, 2000, 2(3), 21–41.

[42] Saltyte-Benth, J., Benth, F. E., A critical view on temperature modelling for application in weather derivatives markets, Energy Economics, 2012, 34, 592–602.

[43] Schiller, F., G. Seidler, Wimmer, M., Temperature models for pricing weather derivatives, Quantitative Finance, 2012, 12(3), 489–500.

[44] Svec, J., Stevenson, M., Modelling and forecasting temperature based weather derivatives, Global Finance Journal, 2007, 18(2), 185–204.

[45] The Economist Magazine, Weather derivatives: Come rain or shine, 2012, `http://www.economist.com/node/21546019`.

[46] Turvey, C.G., Weather derivatives for specific event risks in agriculture, Review of Agricultural Economics, 2001, 23(2), 333–351.

[47] Woodard, J.D., Garcia, P., Weather derivatives, spatial aggregation, and systemic risk: Implications for reinsurance hedging, Journal of Agricultural and Resource Economics, 2008, 33.

Appendix B: Proofs of Theorems

Proof of Theorem 1: We first consider the inner minimization problem in P_{rob} under the ellipsoidal uncertainty set

$$\begin{aligned}
\min_{\tilde{\varepsilon}_{it}} \quad & \sum_{i=1}^{m}\sum_{t=1}^{T} x_i^h p_i^h \gamma_{it} + x_i^c p_i^c \delta_{it} \\
\text{s.t.} \quad & \gamma_{it} \geq r_i - s_{it} - \sum_{k=1}^{3} A_{it}^k \left(H_{i(1-k)} - s_{i(1-k)}\right) - \sum_{k=1}^{t} A_{i(t-k)}^1 \rho_{it} \sum_{j=1}^{m} \sigma_{ij}\tilde{\varepsilon}_{jk}, \quad i=1,\cdots,m, \;\; t=1,\cdots,T \\
& \delta_{it} \geq s_{it} + \sum_{k=1}^{3} A_{it}^k \left(H_{i(1-k)} - s_{i(1-k)}\right) + \sum_{k=1}^{t} A_{i(t-k)}^1 \rho_{it} \sum_{j=1}^{m} \sigma_{ij}\bar{\varepsilon}_{ij}^{\bar{k}} - r_i, \quad i=1,\cdots,m, \;\; t=1,\cdots,T \\
& \|\tilde{\varepsilon}_t\|_2 \leq \kappa, \qquad\qquad t=1,\cdots,T \\
& \gamma_{it}, \delta_{it} \geq 0, \qquad\qquad i=1,\cdots,m, \;\; t=1,\cdots,T
\end{aligned}$$

Let $\alpha_{\mathbf{t}}, \beta_{\mathbf{t}} \in R^m$ and λ_t for $t=1,\cdots,T$ denote Lagrangian multipliers of the corresponding constraints. The unconstrained minimization problem can be written as

$$\min_{\boldsymbol{\gamma_t},\delta_{\mathbf{t}}\boldsymbol{\alpha_t},\boldsymbol{\beta_t},\boldsymbol{\lambda_t}\geq \mathbf{0}} \sum_{i=1}^{m}\sum_{t=1}^{T} x_i^h p_i^h \gamma_{it} + x_i^c p_i^c \delta_{it} + \lambda_t \left(\|\tilde{\varepsilon}_t\|_2 - \kappa\right) + (\alpha_{it} - \beta_{it}) \left(D_{it} - \sum_{k=1}^{t} A_{i(t-k)}^1 \rho_{it} \sum_{j=1}^{m} \sigma_{ij}\tilde{\varepsilon}_{jk} \right) - \alpha_{it}\gamma_{it} - \beta_{it}\delta_{it}$$

where $D_{it} = r_i - s_{it} - \sum_{k=1}^{3} A_{it}^k \left(H_{i(1-k)} - s_{i(1-k)}\right)$. The first order optimality conditions and complementarity conditions for the unconstrained problem are then derived as

$$\begin{aligned}
& x_i^h p_i^h - \alpha_{it} \geq 0, && i=1,\cdots,m, \;\; t=1,\cdots,T \\
& x_i^c p_i^c - \beta_{it} \geq 0, && i=1,\cdots,m, \;\; t=1,\cdots,T \\
& \|\tilde{\varepsilon}_t\|_2 \leq \kappa, && t=1,\cdots,T \\
& \|\tilde{\varepsilon}_t\|_2^{-1} \lambda_t \sum_{j=1}^{m} \tilde{\varepsilon}_{jt} + \sum_{k=t}^{T} A_{i(t-k)}^1 \rho_{it} \sum_{j=1}^{m} \sigma_{ij} \left(\alpha_{jk} - \beta_{jk}\right) = 0, && i=1,\cdots,m, \;\; t=1,\cdots,T \\
& \lambda_t \left(\|\tilde{\varepsilon}_t\|_2 - \kappa\right) = 0, && t=1,\cdots,T \\
& \alpha_{it} \left(D_{it} - \sum_{k=1}^{t} A_{i(t-k)}^1 \rho_{it} \sum_{j=1}^{m} \sigma_{ij}\tilde{\varepsilon}_{jk} - \gamma_{it} \right) = 0, && i=1,\cdots,m, \;\; t=1,\cdots,T \\
& \beta_{it} \left(-D_{it} + \sum_{k=1}^{t} A_{i(t-k)}^1 \rho_{it} \sum_{j=1}^{m} \sigma_{ij}\tilde{\varepsilon}_{jk} - \delta_{it} \right) = 0, && i=1,\cdots,m, \;\; t=1,\cdots,T.
\end{aligned}$$

From the first complementarity condition, we obtain $\|\tilde{\varepsilon}_t\|_2 - \kappa = 0$ since $\lambda_t \neq 0$ for $t=1,\cdots,T$. For the sake of simplicity, let $\mathbf{B}_t$ denote a vector that is consisting of $B_t(i) = \sum_{k=t}^{T} \left(\alpha_{ik} - \beta_{ik}\right) A_{i(t-k)}^1 \rho_{it}$ for $t=1,\cdots,T$ and $i=1,\cdots,m$. Thus, the solution of the optimality conditions provides the worst-case values of the random variables varying in the ellipsoidal uncertainty set as $\tilde{\varepsilon}_t = -\frac{\kappa}{\lambda_t} \boldsymbol{\Sigma_t} \mathbf{B_t}$ and we obtain $\lambda_t = \|\boldsymbol{\Sigma_t} \mathbf{B_t}\|_2$.

In addition, the objective function value of the unconstrained optimization problem is

$$\sum_{i=1}^{m}\sum_{t=1}^{T}(\alpha_{it}-\beta_{it})\left(r_i-s_{it}-\sum_{k=1}^{3}A_{it}^{k}\left(H_{i(1-k)}-s_{i(1-k)}\right)\right)-\kappa\left\|\mathbf{\Sigma_t}\mathbf{B}_t\right\|_2$$

Re-injection of the KKT conditions and the worst-case uncertain parameters into P_{rob} leads to the robust counterpart of the portfolio allocation problem under the ellipsoidal uncertainty set as stated in Theorem 1.

Proof of Theorem 2: The inner minimization problem in P_{rob} under the asymmetric uncertainty set,

$$\begin{aligned}
\min_{\tilde{\mathbf{v}}_\mathbf{t},\tilde{\mathbf{w}}_\mathbf{t},\gamma_\mathbf{t},\delta_\mathbf{t}} \quad & \sum_{i=1}^{m}\sum_{t=1}^{T}x_i^h p_i^h\gamma_{it}+x_i^c p_i^c\delta_{it} \\
s.t. \quad & \gamma_{it}\geq r_i-s_{it}-\sum_{k=1}^{3}A_{it}^{k}\left(H_{i(1-k)}-s_{i(1-k)}\right)-\sum_{k=1}^{t}A_{i(t-k)}^{1}\rho_{it}\sum_{j=1}^{m}\sigma_{ij}\left(\tilde{v}_{jk}-\tilde{w}_{jk}\right), \\
& \qquad\qquad i=1,\cdots,m,\quad t=1,\cdots,T \\
& \delta_{it}\geq s_{it}+\sum_{k=1}^{3}A_{it}^{k}\left(H_{i(1-k)}-s_{i(1-k)}\right)+\sum_{k=1}^{t}A_{i(t-k)}^{1}\rho_{it}\sum_{j=1}^{m}\sigma_{ij}\left(\tilde{v}_{jk}-\tilde{w}_{jk}\right)-r_i, \\
& \qquad\qquad i=1,\cdots,m,\quad t=1,\cdots,T \\
& \left\|\mathbf{P}^{-1}\tilde{\mathbf{v}}_\mathbf{t}+\mathbf{R}^{-1}\tilde{\mathbf{w}}_\mathbf{t}\right\|_2\leq\Omega, \qquad t=1,\cdots,T \\
& \tilde{\mathbf{v}}_\mathbf{t},\tilde{\mathbf{w}}_\mathbf{t},\gamma_\mathbf{t},\delta_\mathbf{t}\geq 0, \qquad t=1,\cdots,T
\end{aligned}$$

can be rewritten as the following unconstrained minimization problem

$$\begin{aligned}
\min_{\tilde{\mathbf{v}}_\mathbf{t},\tilde{\mathbf{w}}_\mathbf{t},\gamma_\mathbf{t},\delta_\mathbf{t},\alpha_\mathbf{t},\beta_\mathbf{t},\lambda_\mathbf{t}\geq\mathbf{0}} \quad & \sum_{i=1}^{m}\sum_{t=1}^{T}(x_i^h p_i^h-\alpha_{it})\gamma_{it}+(x_i^c p_i^c-\beta_{it})\delta_{it}+\lambda_t\left(\left\|\mathbf{P}^{-1}\tilde{\mathbf{v}}_\mathbf{t}+\mathbf{R}^{-1}\tilde{\mathbf{w}}_\mathbf{t}\right\|_2-\Omega\right) \\
& +(\alpha_{it}-\beta_{it})\left(D_{it}-\sum_{k=1}^{t}A_{t-k}^{1}\rho_{it}\sum_{j=1}^{m}\sigma_{ij}\left(\tilde{v}_{jk}-\tilde{w}_{jk}\right)\right)
\end{aligned}$$

where $\alpha_\mathbf{t},\beta_\mathbf{t}\in R^m$ and λ_t for $t=1,\cdots,T$ are Lagrangian multipliers for the corresponding constraints and $D_{it}=r_i-s_{it}-\sum_{k=1}^{3}A_{it}^{k}\left(H_{i(1-k)}-s_{i(1-k)}\right)$. It is worthwhile to mention that $\tilde{v}_{it}\tilde{w}_{it}=0$, and ϕ_i^{-1} and ψ_i^{-1} are i-th diagonal elements of matrices $\mathbf{P}^{-1}$ and $\mathbf{R}^{-1}$, respectively. The worst-case values of $\tilde{v}_{it}$ and $\tilde{w}_{it}$ within the asymmetric uncertainty set can be obtained by solving the KKT optimality conditions. From the complementarity conditions, $\lambda_t\left(\left\|\mathbf{P}^{-1}\tilde{\mathbf{v}}_\mathbf{t}+\mathbf{R}^{-1}\tilde{\mathbf{w}}_\mathbf{t}\right\|_2-\Omega\right)=0$, a trivial solution is obtained only if $\lambda_t=0$. When $\lambda_t\neq 0$, then $\left\|\mathbf{P}^{-1}\tilde{\mathbf{v}}_\mathbf{t}+\mathbf{R}^{-1}\tilde{\mathbf{w}}_\mathbf{t}\right\|_2-\Omega=0$. In this case, the first order derivatives of the Lagrangian function (of the original problem) with respect to $\tilde{v}_{it}$ and $\tilde{w}_{it}$ for $i=1,\cdots,m$ and $t=1,\cdots,T$ are

$$\begin{aligned}
&\left\|\mathbf{P}^{-1}\tilde{\mathbf{v}}_\mathbf{t}+\mathbf{R}^{-1}\tilde{\mathbf{w}}_\mathbf{t}\right\|^{-1}\lambda_t\left(\sum_{j=1}^{m}\phi_i^{-1}\phi_j^{-1}\tilde{v}_{jt}+\phi_i^{-1}\psi_j^{-1}\tilde{w}_{jt}\right)-\sum_{k=1}^{t}A_{i(t-k)}^{1}\rho_{it}\sum_{j=1}^{m}\sigma_{ij}\left(\alpha_{jk}-\beta_{it}\right)\geq 0, \\
&\left\|\mathbf{P}^{-1}\tilde{\mathbf{v}}_\mathbf{t}+\mathbf{R}^{-1}\tilde{\mathbf{w}}_\mathbf{t}\right\|^{-1}\lambda_t\left(\sum_{j=1}^{m}\phi_i^{-1}\psi_j^{-1}\tilde{v}_{jt}+\psi_i^{-1}\psi_j^{-1}\tilde{w}_{jt}\right)+\sum_{k=1}^{t}A_{i(t-k)}^{1}\rho_{it}\sum_{j=1}^{m}\sigma_{ij}\left(\alpha_{jk}-\beta_{it}\right)\geq 0.
\end{aligned}$$

These inequalities can be further simplified as

$$\begin{aligned}
&\frac{\lambda_t}{\Omega}\phi_i^{-2}\tilde{v}_{it} + \frac{\lambda_t}{\Omega}\phi_i^{-1}\psi_i^{-1}\tilde{w}_{it} \geq \sum_{k=1}^{t} A^1_{i(t-k)}\rho_{it}\sum_{j=1}^{m}\sigma_{ij}\left(\alpha_{jk}-\beta_{it}\right)\\
&\frac{\lambda_t}{\Omega}\phi_i^{-1}\psi_i^{-1}\tilde{v}_{it} + \frac{\lambda_t}{\Omega}\psi_i^{-2}\tilde{w}_{it} \geq -\sum_{k=1}^{t} A^1_{i(t-k)}\rho_{it}\sum_{j=1}^{m}\sigma_{ij}\left(\alpha_{jk}-\beta_{it}\right)
\end{aligned} \tag{8}$$

Since both γ_{it} and δ_{it} are nonnegative, at most one of the Lagrangian multipliers α_{jk} and β_{it} can be non-zero. For $\alpha_{jk}=0$, the inequalities in (8) become

$$\begin{aligned}
\frac{\lambda_t}{\Omega}\left(\phi_i^{-2}\tilde{v}_{it} + \phi_i^{-1}\psi_i^{-1}\tilde{w}_{it}\right) &\geq -\sum_{k=1}^{t} A^1_{i(t-k)}\rho_{it}\sum_{j=1}^{m}\sigma_{ij}\beta_{it},\\
\frac{\lambda_t}{\Omega}\left(\phi_i^{-1}\psi_i^{-1}\tilde{v}_{it} + \psi_i^{-2}\tilde{w}_{it}\right) &\geq \sum_{k=1}^{t} A^1_{i(t-k)}\rho_{it}\sum_{j=1}^{m}\sigma_{ij}\beta_{it}.
\end{aligned}$$

In this case, if $\tilde{v}_{it}=0$, then $\frac{\lambda_t}{\Omega}\psi_i^{-2}\tilde{w}_{it} \geq \sum_{k=1}^{t} A^1_{i(t-k)}\rho_{it}\sum_{j=1}^{m}\sigma_{ij}\beta_{it}$. On the other hand, when $\tilde{w}_{it}=0$, one achieves $\frac{\lambda_t}{\Omega}\phi_i^{-1}\psi_i^{-1}\tilde{v}_{it} \geq \sum_{k=1}^{t} A^1_{i(t-k)}\rho_{it}\sum_{j=1}^{m}\sigma_{ij}\beta_{it}$. Similarly, one can easily see that when $\beta_{it}=0$, the inequalities in (8) become

$$\frac{\lambda_t}{\Omega}\phi_i^{-2}\tilde{v}_{it} \geq \sum_{k=1}^{t} A^1_{i(t-k)}\rho_{it}\sum_{j=1}^{m}\sigma_{ij}\alpha_{jk}, \text{ and } \frac{\lambda_t}{\Omega}\phi_i^{-1}\psi_i^{-1}\tilde{w}_{it} \geq \sum_{k=1}^{t} A^1_{i(t-k)}\rho_{it}\sum_{j=1}^{m}\sigma_{ij}\alpha_{jk}.$$

that can be further simplified as

$$\tilde{w}_{it} \geq \frac{\Omega}{\lambda_t}\psi_i^2\sum_{k=1}^{t} A^1_{i(t-k)}\rho_{it}\sum_{j=1}^{m}\sigma_{ij}\left(\alpha_{jk}+\beta_{it}\right), \text{ and } \tilde{v}_{it} \geq \frac{\Omega}{\lambda_t}\phi_i^2\sum_{k=1}^{t} A^1_{i(t-k)}\rho_{it}\sum_{j=1}^{m}\sigma_{ij}\left(\alpha_{jk}+\beta_{it}\right)$$

The unconstrained optimization problem can be rewritten as

$$\sum_{i=1}^{m}\sum_{t=1}^{T}\left(r_i - s_{it} - \sum_{k=1}^{3} A^k_{it}\left(H_{i(1-k)} - s_{i(1-k)}\right)\right)\left(\alpha_{it}-\beta_{it}\right) + \sum_{k=t}^{T} A^1_{(t-k)}\rho_{it}\sigma_{ij}\left(\alpha_{it}-\beta_{it}\right)\left(\tilde{v}_{ik}-\tilde{w}_{ik}\right)$$

The initial minimization problem becomes

$$\begin{aligned}
\inf\quad & \sum_{i=1}^{m}\sum_{t=1}^{T}\left(r_i - s_{it} - \sum_{k=1}^{3} A^k_{it}\left(H_{i(1-k)} - s_{i(1-k)}\right)\right)\left(\alpha_{it}-\beta_{it}\right) + \sum_{k=t}^{T} A^1_{i(t-k)}\rho_{it}\sigma_{ij}\left(\alpha_{it}-\beta_{it}\right)\left(\tilde{v}_{ik}-\tilde{w}_{ik}\right)\\
\text{s.t}\quad & \tilde{w}_{it} \geq -\frac{\Omega}{\lambda_t}\psi_i^2\sum_{k=1}^{t} A^1_{i(t-k)}\rho_{it}\sum_{j=1}^{m}\sigma_{ij}\left(\alpha_{jt}+\beta_{it}\right), \qquad \tilde{w}_{it}\geq 0, \qquad i=1,\cdots,m, \quad t=1,\cdots,T\\
& \tilde{v}_{it} \geq \frac{\Omega}{\lambda_t}\phi_i^2\sum_{k=1}^{t} A^1_{i(t-k)}\rho_{it}\sum_{j=1}^{m}\sigma_{ij}\left(\alpha_{jt}+\beta_{it}\right), \qquad \tilde{v}_{it}\geq 0, \qquad i=1,\cdots,m, \quad t=1,\cdots,T\\
& \left\| \mathbf{P^{-1}}\tilde{\mathbf{v}}_\mathbf{t} + \mathbf{R^{-1}}\tilde{\mathbf{w}}_\mathbf{t}\right\| = \Omega
\end{aligned}$$

Using the proposition in Chen et. al (2008), the optimal solution of this problem is obtained as

$$\sum_{i=1}^{m}\sum_{t=1}^{T}\left(r_i - s_{it} - \sum_{k=1}^{3} A_{it}^{k}\left(H_{i(1-k)} - s_{i(1-k)}\right)\right)(\alpha_{it} - \beta_{it}) - \Omega\sum_{k=1}^{t}\|u_k\|_2$$

$$u_{it} \geq \phi_i \sum_{k=1}^{t} A_{i(t-k)}^{1}\rho_{it}\sum_{j=1}^{m}\sigma_{ij}\left(\alpha_{jk} + \beta_{it}\right), \qquad i = 1,\cdots,m,\ t = 1,\cdots,T$$

$$u_{it} \geq \psi_i \sum_{k=1}^{t} A_{i(t-k)}^{1}\rho_{it}\sum_{j=1}^{m}\sigma_{ij}\left(\alpha_{jk} + \beta_{it}\right), \qquad i = 1,\cdots,m,\ t = 1,\cdots,T$$

$$u_{it} \geq 0, \qquad i = 1,\cdots,m,\ t = 1,\cdots,T$$

Re injecting these into R_{rob}, the robust counterpart of portfolio allocation problem under the asymmetric uncertainty set R_{asym} is derived as stated in Theorem 2.